6.11 Atmospheric CO_2 and O_2 During the Phanerozoic: Tools, Patterns, and Impacts

DL Royer, Wesleyan University, Middletown, CT, USA

6.11.1 Introduction

The partial pressures of CO_2 and O_2 impart a first-order control on Earth's climatic and biotic systems. CO_2 is an important greenhouse gas and is a fundamental building block for most life, while O_2 is intimately linked to metabolism. The levels of these two critical gases are not static: their temporal variability over millennial and longer timescales has been long noted (Beerling, 2007; Lane, 2002; Weart, 2003). This temporal behavior potentially offers tremendous explanatory power for making sense of the geologic record. For example, over a century ago, Arrhenius (1896) and Chamberlin (1897, 1898, 1899) argued for the importance of CO_2 in regulating global climate over geologic timescales. In recent decades, attention has also been turned to the two-way interplay over time between life and atmospheric composition (e.g., Beerling, 2007), for example, how the evolution of forests may have facilitated insect gigantism via atmospheric O_2 (**Section 6.11.4.2**). Equally important, studies of the ancient Earth system, including paleoclimate, have increasingly been used as analogues to help predict the future trajectory of the current Earth system (e.g., IPCC, 2007).

The goal of this review is to describe the major model- and proxy-based approaches for reconstructing pre-Pleistocene CO_2 and O_2, including their limitations, and to present several geologic case studies that highlight the impacts of CO_2 and O_2 on climate and life. The review is not exhaustive and focuses mainly on developments within the last decade.

6.11.2 Models for Atmospheric CO_2 and O_2 Estimation

6.11.2.1 Key Principles

The flow of CO_2 and O_2 into and out of the atmosphere over multimillion-year timescales is largely controlled by a handful of processes (**Figure 1**). These processes primarily act to transfer CO_2 and O_2 between rocks and surficial reservoirs (atmosphere, ocean, and land surfaces). Critically, if the rate of the processes over time can be determined, then the geologic trajectories of CO_2 and O_2 can be quantified.

The key processes were enumerated in 1845 by French chemist and mining engineer J.J. Ebelmen (1845; see also Berner and Maasch, 1996), with more modern treatments given by Urey (1952), Garrels and Perry (1974), Holland (1978), Walker et al. (1981), Berner et al. (1983), Garrels and Lerman (1984), Berner and Canfield (1989), and Berner (1991, 2004). There are two main sinks for CO_2 over multimillion-year timescales. The first is the formation and burial of carbonates whose ionic components (Ca^{2+}, Mg^{2+}, and HCO_3^-) derive from the weathering of Ca and Mg silicate rocks. Carbonate formation releases a stoichiometrically

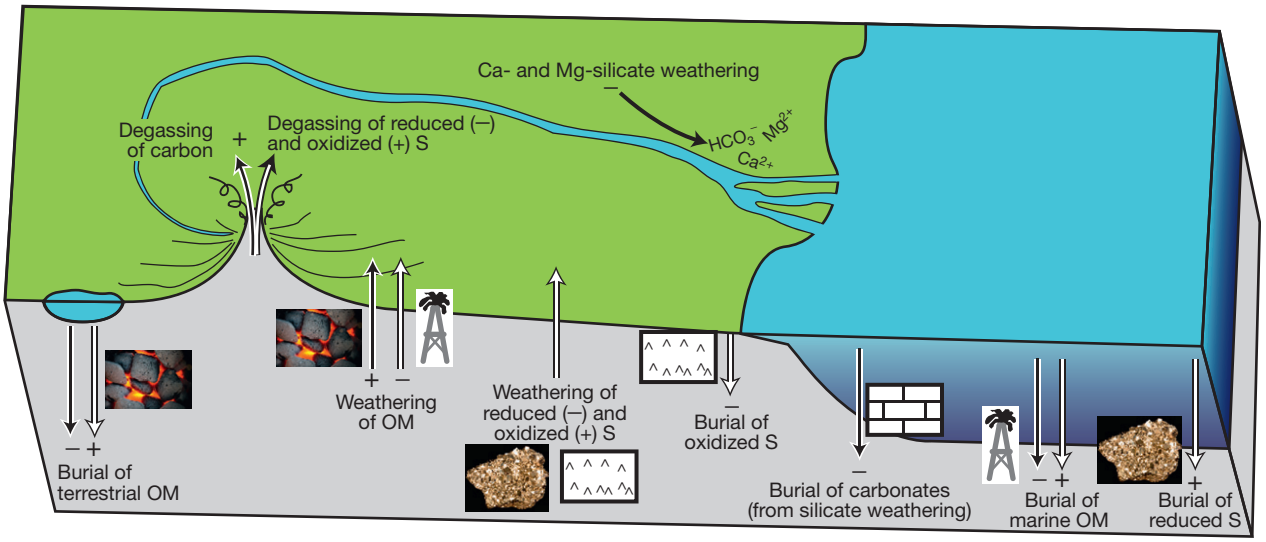

Figure 1 Major processes that control the long-term evolution of atmospheric CO_2 (black arrows) and O_2 (white arrows). Arrows linked to plus signs (+) cause an increase in the gas concentration, while those with minus signs (−) cause a decrease.

equivalent amount of CO_2, but the weathering of one mole of silicate mineral consumes two moles of HCO_3^-. Thus, assuming no large, long-term change in ocean alkalinity (Holland, 1984), the weathering of Ca and Mg silicate rocks consumes a stoichiometrically equivalent amount of CO_2:

Weathering of a generalized calcium silicate:

$$2CO_2 + H_2O + CaSiO_3 \rightarrow Ca^{2+} + 2HCO_3^- + SiO_2 \quad [1]$$

Precipitation of calcium carbonate:

$$Ca^{2+} + 2HCO_3^- \rightarrow CaCO_3 + CO_2 + H_2O \quad [2]$$

Sum of eqns [1] and [2]:

$$CO_2 + CaSiO_3 \rightarrow CaCO_3 + SiO_2 \quad [3]$$

The second major sink for CO_2 is the burial of organic matter (on land or in the ocean). This burial process physically separates the carbon from the surface Earth system until, tens to hundreds of millions of years later, tectonic forces return the carbon to the atmosphere via degassing or direct chemical weathering (respiration) of organic-rich rocks. Because the formation of organic matter also involves the release of O_2, the burial of organic matter leads to the buildup of atmospheric O_2 and its weathering (oxidation) to O_2 consumption. These processes can be conceptualized as 'geo'-photosynthesis (eqn [4] from left to right) and 'geo'-respiration (eqn [4] from right to left):

$$CO_2 + H_2O \leftrightarrow CH_2O + O_2 \quad [4]$$

The cycling of sulfur between rocks and the surface Earth also impacts atmospheric O_2. This is because the dominant pathway for reducing sulfur is through sulfur-reducing bacteria, who metabolize organic matter without consuming oxygen. If the reduced sulfur is then buried (typically as pyrite, FeS_2), then the O_2 that was released when the associated organic matter was synthesized remains in the atmosphere. Over long timescales, this can lead to the buildup of atmospheric O_2:

$$2Fe_2O_3 + 8SO_4^{2-} + 16H^+ \leftrightarrow 15O_2 + 4FeS_2 + 8H_2O \quad [5]$$

Similarly, if oxidized sulfur enters the rock reservoir (typically as gypsum, $CaSO_4$), then this can lead to a drawdown of O_2 because less sulfur is available for pyrite formation. When reduced sulfur is released into the surface Earth system via degassing or direct pyrite weathering, oxygen is consumed via oxidation (eqn [5] from right to left). For opposite reasons, the return of oxidized sulfur to the surface Earth leads to the retention of atmospheric O_2. During the Phanerozoic, the sulfur cycle is typically secondary to the organic carbon cycle for impacting O_2, but the effects are nevertheless nonnegligible (Berner, 2004).

It is clear from this discussion that the long-term controls of atmospheric CO_2 and O_2 are linked via the carbon cycle. For processes related to the cycling of organic matter, there are opposing but stoichiometrically equivalent impacts on CO_2 and O_2. The burial of organic matter leads to a drop in CO_2 and equal rise in O_2, and vice versa for organic-matter weathering. It may be expected, then, that CO_2 and O_2 show opposing patterns over time. However, other processes only impact CO_2 (e.g., silicate weathering) or O_2 (e.g., pyrite formation). Thus, changes in CO_2 and O_2 can be decoupled.

The processes that control the long-term evolution of CO_2 and O_2 are distinct from their short-term control. Most noticeably, the more familiar short-term carbon cycle, which involves the transfer of carbon within the surface Earth system, is not directly relevant to the long-term control of atmospheric CO_2 and O_2. This is because any large change in the size of these reservoirs (e.g., soil, marine inorganic carbon) cannot be sustained over geologically relevant timescales. Over long timescales, these reservoirs can be assumed to be in quasi steady state (Berner, 2004). As a result, the short-term carbon cycle dominates the control of atmospheric CO_2 over timescales of approximately $<10^3$ years and the long-term carbon cycle for timescales of $>10^5$ years.

6.11.2.2 GEOCARB Models

Berner et al. (1983) and Berner and Canfield (1989) applied the principles described in **Section 6.11.2.1** to quantify

multimillion-year patterns in CO_2 and O_2, respectively. Berner and colleagues have since expanded and refined these original studies (Berner, 1991, 1994, 2001, 2004, 2006a,c, 2008, 2009; Berner and Kothavala, 2001; Berner et al., 2000). The model began as GEOCARB, a model for Phanerozoic CO_2 based only on the long-term carbon cycle, and subsequently evolved to its latest iteration, GEOCARBSULFvolc, a model for CO_2 and O_2 based on both the carbon and sulfur cycles. The discussion here is based mainly on GEOCARBSULFvolc.

Critical for the GEOCARB family of models is the correct parameterization of the processes described earlier (**Section 6.11.2.1**). In other words, how have the burial, weathering, and degassing fluxes changed over time? The overarching framework of the model is an isotopic mass balance, where the mass and stable isotopic composition of carbon and sulfur in the surface Earth system at a given time in the past is related to the flux and isotopic values of carbon and sulfur moving into and out of the system (Berner, 2004). Tracking isotopes are helpful because many of the major reservoirs (**Figure 1**) have distinct values.

6.11.2.2.1 Silicate weathering

The chemical weathering of Ca and Mg silicates has received considerable attention because it is a key, negative climate feedback for maintaining long-term global temperatures within a narrow range (Berner et al., 1983; Pagani et al., 2009; Walker et al., 1981; Zeebe and Caldeira, 2008; see also **Chapter 6.15**). Both CO_2 and temperature impact chemical weathering rates: these effects have been documented in field studies (Andrews and Schlesinger, 2001; Baars et al., 2008; Gislason et al., 2009) and for events in the geological past (Dallanave et al., 2010). Temperature is inferred partly via climate sensitivity to CO_2; a value of 3 °C per CO_2 doubling is typical, but estimates of higher climate sensitivity, especially for glacial periods (Hansen et al., 2008; Pagani et al., 2010; Park and Royer, 2011; see also **Section 6.11.4.1**), may call for a re-parameterization (Berner, 2004). Changing paleogeography, for example, changing land area or poleward drift of a continent (Worsley and Kidder, 1991), also affects weathering. Proper treatment of this factor requires coupling paleogeographic reconstructions with climate model simulations (e.g., Otto-Bliesner, 1995); some progress in this area has been made (Donnadieu et al., 2006a; Le Hir et al., 2011).

Vegetation strongly impacts rock weathering rate by acidifying the soil, increasing soil moisture, and lengthening water–mineral contact time (Berner, 1992). Vegetation factors presently considered in GEOCARB are the transition from a minimally vegetated to forested land surface and the transition from gymnosperms to angiosperms (Baars et al., 2008; Moulten and Berner, 1998; Moulton et al., 2000). Another possible important factor that is presently excluded is the mycorrhizal associations (Taylor et al., 2009). These vegetation processes are some of the least constrained in GEOCARB and are responsible for considerable uncertainty in the CO_2 calculations (Berner, 2004; Berner and Kothavala, 2001).

Mean continental relief affects chemical weathering via the confounding influence of physical erosion and runoff. This relief factor has been estimated via strontium isotopes and abundance of sedimentary rocks (Berner, 2004). Also, because volcanic rocks weather more quickly than nonvolcanic silicate rocks, their changing proportions over time are incorporated (Berner, 2006c, 2008; Wallmann, 2001).

6.11.2.2.2 Weathering of carbonates, organic matter, pyrite, and gypsum

The weathering of carbonates, organic matter, pyrite, and sulfate minerals is treated in a manner similar to silicate weathering (**Section 6.11.2.2.1**), but with different rate constants. Factors for carbonate and organic matter weathering include uplift (runoff), paleogeography (and its climatic consequences), and land area. Some carbon-cycle models include an O_2 dependency for organic matter weathering (e.g., Bergman et al., 2004), but this dependency is typically weak (Bolton et al., 2006; Wildman et al., 2004a). For carbonates, factors related to plant evolution and the direct weathering effect of CO_2 and temperature are also included. The weathering of pyrite is linked to land area (calculated from rock abundances and associated reduced sulfur contents of marine and coal basin sediments) and uplift, while the weathering of gypsum is linked to sulfate abundance and the paleogeographic impact on climate (because sulfate minerals are highly soluble) (Berner, 2006a).

A final modifying parameter is related to the observation that younger rocks are more likely to weather than older rocks because they tend to be closer to the Earth's surface ('rapid recycling'; Garrels and Mackenzie, 1971). In GEOCARB, the relative proportions of two age classes (young and old) are computed from rock abundance data.

6.11.2.2.3 Burial of organic matter and pyrite

The burial flux of organic matter is estimated in two ways (Berner, 2004): through rock abundance data and their associated organic carbon contents and through the carbon isotopic history of shallow marine carbonates, which serve as a proxy for the atmosphere. Because the $\delta^{13}C$ of organic matter is distinctly more negative than the atmosphere, an increased burial flux causes an isotopic enrichment in the atmosphere and oceans. Such an enrichment is clearly seen during the Carboniferous and Permian (Prokoph et al., 2008; Veizer et al., 1999). An additional factor is included to account for the O_2 dependency on the carbon isotopic fractionation during photosynthesis (both for plants and phytoplankton) (Beerling et al., 2002b; Berner, 2009; Berner et al., 2000; Berry et al., 1972).

Pyrite burial has also been modeled from both rock abundance data and the sulfur isotopic history of sulfate in shallow marine carbonates, which, as with carbon, serve as an atmospheric proxy. The biologically mediated process of pyrite formation incorporates isotopically depleted sulfur, meaning an increased burial flux in pyrite leads to an isotopic enrichment in the atmosphere and oceans. A modifying parameter to account for the inverse effect of atmospheric O_2 on the isotopic fractionation of sulfur is included (Berner, 2001; Berner et al., 2000).

For both organic matter and pyrite burial, the two approaches (mass balance and isotopic mass balance) yield similar estimates of O_2 (Berner, 2001, 2004; Berner et al., 2000).

6.11.2.2.4 Degassing

CO_2 degassing from volcanic, metamorphic, and diagenetic processes is one of the least-constrained components of long-term carbon cycle models (Berner, 2004). Seafloor spreading

rates are often considered a proxy for degassing (e.g., Berner et al., 1983). Spreading rates can be inferred from the volume of intact seafloor (Seton et al., 2009) and, for times predating intact seafloor (>180 Ma), from global sea level (Gaffin, 1987). Kerrick (2001) considers this approach too simplified and instead proposes that global degassing scales more directly with volcanic rock volume. Following this approach, Berner (2004) found no first-order disagreement with the spreading rate approach.

Before 150 Ma, deep-sea carbonate formation was rare because most calcareous plankton had not yet evolved (Wilkinson and Walker, 1989). Because deep-sea sediment is more likely to be subducted than sediment deposited on shelves, the evolutionary radiation of calcareous plankton likely influenced degassing (Ridgwell and Zeebe, 2005). In GEOCARB, the effect is modeled as a linear increase in subducted carbonate beginning at 150 Ma (Berner, 1994).

6.11.2.2.5 Estimates of CO_2 and O_2 from the GEOCARB model

Following the parameterizations outlined earlier (Sections 6.11.2.2.1–6.11.2.2.4), the Phanerozoic histories of atmospheric CO_2 and O_2 can be computed (Figure 2). These are computed in units of mass abundance (i.e., partial pressure), but for convenience have been converted here to volumetric fraction (ppm) assuming unity at sea level (e.g., a doubling in mass equals a doubling in volumetric fraction). CO_2 was high (above 2000 ppm) for much of the early Paleozoic, followed by a precipitous drop to present-day levels (<500 ppm) near the end of the Devonian. This CO_2 drop was triggered largely by the origin and expansion of forests, which increased chemical weathering rates (Section 6.11.2.2.1) and permitted increased burial of organic carbon (Section 6.11.2.2.3). Increased degassing (Section 6.11.2.2.4) led to elevated CO_2 levels during the Cretaceous (~1000 ppm), followed by a steady decline to the present day (Figure 2(a)), due in part to relief-driven changes in silicate weathering.

Atmospheric O_2 levels oscillated between 15% and 25% for much of the Phanerozoic, with one large, positive excursion to >30% centered on the late Carboniferous and Permian (Figure 2(b)). This spike was largely caused by an increase in organic carbon burial (see also Section 6.11.4.2).

6.11.2.3 Other Models for CO_2 and O_2 Reconstruction

There are other long-term geochemical models that calculate Phanerozoic CO_2 and O_2. Most are grounded in the principles outlined earlier (Section 6.11.2.1) and thus share many traits with the GEOCARB family of models. For example, Budyko et al. (1987) track the mass abundance of carbon- and sulfur-bearing rocks much like GEOCARB, but they do not incorporate isotopes and include fewer modifying parameters. Their CO_2 and O_2 calculations are similar to GEOCARB except for lower CO_2 during the Cambrian–Silurian and an additional large O_2 spike during the Cretaceous.

Falkowski et al. (2005) use the oxygen model of Berner (2001) and updated sulfur and carbon isotope records to reconstruct atmospheric O_2 for the past 205 My. Tajika (1998) and Kashiwagi and Shikazono (2003) model CO_2 for the last 150 and 65 My, respectively, in a manner similar to GEOCARB except for expanded treatments of degassing. The results from these three models broadly match those from GEOCARB. Wallmann (2001, 2004) developed a set of independent GEOCARB-style models, with an additional focus on the submarine weathering of basalt. However, most studies point to submarine weathering having only a minor role in long-term CO_2 control (see Berner, 2004 for summary). In Wallmann (2004), reconstructions of galactic cosmic radiation modify the temperature inputs; however, cosmic ray reconstructions and their possible impact on climate are poorly understood (Rahmstorf et al., 2004; Royer et al., 2004).

Three models have expanded beyond the carbon–oxygen–sulfur system to include other elements, such as phosphorus and iron (Arvidson et al., 2006; Bergman et al., 2004; Hansen and Wallmann, 2003). This allows for the inclusion of more feedback processes, for example, the negative feedback between atmospheric O_2 and marine P via organic matter burial (Van Cappellen and Ingall, 1996).

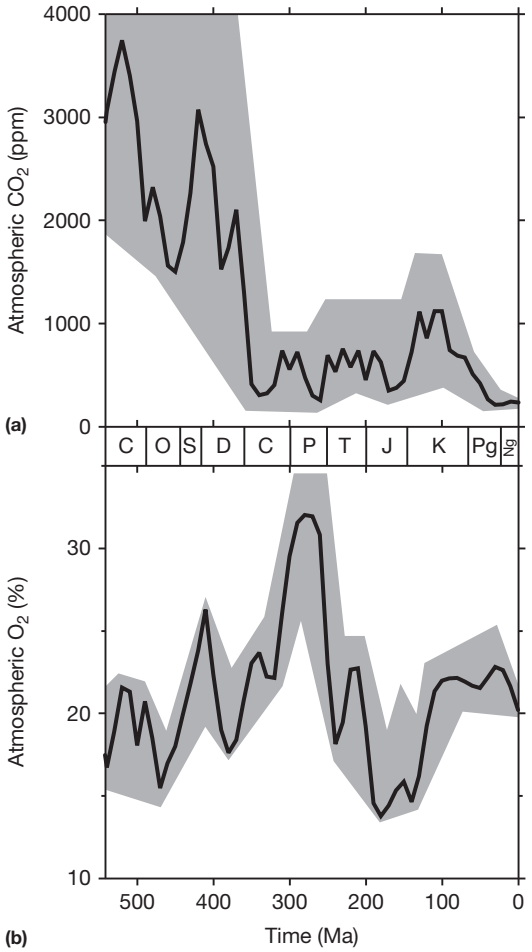

Figure 2 Phanerozoic history of atmospheric CO_2 and O_2 from the GEOCARBSULFvolc model. CO_2 history is from Berner (2008), assuming a basalt/granite weathering rate ratio (VNV) of 5, a present-day basalt–seawater reaction rate (fB(0)) of 4, and a strontium isotope variability in granites over time (NV) of 0.015. The error envelope, which captures the likely range of the input parameters, is updated from Berner and Kothavala (2001). O_2 history is from Berner (2009). The error envelope is updated from Berner (2006a).

Most long-term carbon- and oxygen-cycle models have coarse time resolution. The GEOCARB model, for example, typically has a 10 My time step. An obvious drawback to this approach is that short-term events, such as the Paleocene–Eocene thermal maximum and the K–T boundary bolide impact, are not captured. However, a coarse time resolution is not intrinsic to these models; it simply reflects the difficulty in resolving processes, such as runoff and chemical weathering, especially during the Paleozoic and early Mesozoic. While no high-resolution model exists yet for the entire Phanerozoic, there are some high-resolution models for targeted intervals (e.g., Berner, 2005; Gibbs et al., 1997; Saltzman et al., 2011; Tajika, 1998).

Other models emphasize one aspect of long-term geochemical cycles. For example, the GEOCLIM model is a GEOCARB-style model for CO_2 estimation but with a sophisticated, spatially resolved module for silicate weathering (Donnadieu et al., 2006b, 2009; Goddéris et al., 2008; Le Hir et al., 2011). Clearly, there is simultaneous movement in long-term geochemical models to shorten time steps and to more completely describe the processes that control the long-term evolution of CO_2 and O_2.

6.11.3 Proxies for Atmospheric Reconstruction

Atmospheric CO_2 and O_2 cannot be measured directly for the pre-Pleistocene. However, CO_2 and O_2 covary with many elements in the Earth system today, and some of these elements can be measured in rocks. These proxies provide an alternative approach for reconstructing CO_2 and O_2 that are independent from geochemical models. The foundational caveat for all proxies is the uniformitarian assumption that their governing processes have not changed over time.

There has been an explosion of paleo-CO_2 proxies over the past two decades. The six leading methods are described here (**Sections 6.11.3.1–6.11.3.5**). Proxies for atmospheric O_2, while less quantitative, are described too (**Section 6.11.3.7**). In both cases, recent developments are emphasized. More exhaustive reviews can be found elsewhere (Berner et al., 2003; Freeman and Pagani, 2005; Pagani, 2002; Royer, 2001; Royer et al., 2001a; Sheldon and Tabor, 2009). With the exception of the paleosol proxies (**Section 6.11.3.3**), all CO_2 proxies described here respond to pCO_2; for convenience, all reconstructions are expressed in units of volumetric fraction (ppm) assuming unity at sea level (e.g., a doubling in pressure corresponds to a doubling in volumetric fraction).

6.11.3.1 CO_2: Stomata

Stomata are the microscopic pores on leaf surfaces that facilitate gas exchange with the atmosphere, namely, CO_2, O_2, and H_2O. Approximately 200% and 16% of the total content of atmospheric water vapor and CO_2 are cycled through stomata each year (Hetherington and Woodward, 2003). As such, stomata are finely tuned to the atmosphere. Woodward (1986) demonstrated that stomatal density typically increases with elevation. This response, replicated in experiments (Woodward and Bazzaz, 1988), is largely driven by lower pCO_2 and the plant's requirement to maintain photosynthetic rates but with a transpirational cost (Royer et al., 2001a; Woodward, 1987). Because both atmospheric pressure and atmospheric CO_2 mass affect pCO_2, if pressure is controlled for CO_2, concentration (ppm) can be reconstructed. Typically, stomatal index ($100 \times$ stomatal density/[stomatal density + epidermal cell density]), not stomatal density, is used for CO_2 reconstruction because stomatal index is influenced by fewer environmental factors (Royer, 2001). For example, stomatal density is more sensitive to water potential gradients within leaves and canopies (including sun and shade leaves) because water stress affects epidermal cell size (and thus stomatal density) but not stomatal initiation rates (and thus stomatal index) (Kürschner, 1997; Royer, 2001; Sun et al., 2003). Light intensity affects both stomatal density and stomatal index (Lake et al., 2001); however, in natural forest systems, the impact on stomatal index appears minor (Royer, 2001; Sun et al., 2003).

A strength of the stomatal approach for quantifying paleo-CO_2 is that the genetic (Casson and Gray, 2008; Gray et al., 2000), functional (Kleidon, 2007; Konrad et al., 2008; Wynn, 2003), and signaling (Lake et al., 2001, 2002) pathways that underpin the inverse relationship are fairly well understood. Stomata-based CO_2 reconstructions also compare favorably to coeval estimates from Pleistocene and Holocene ice cores (McElwain et al., 2002; Rundgren and Beerling, 1999, 2003; Rundgren et al., 2005).

The principal limitation of the proxy is that the stomata lose sensitivity at high CO_2 faster than the other proxies (**Figure 3**). Above $\sim$700 ppm, the upper error limits for most stomata-based CO_2 estimates are unbounded. Another constraint on using the stomata to reconstruct CO_2 is that atmospheric pressure needs to be considered. Thus, fossil studies must account for paleoelevation; in most cases, if the paleoelevation of a site is $<$1000 m, then the impact of atmospheric pressure is minor (Beerling and Royer, 2002). The final constraint is that the stomatal responses to CO_2 are commonly species-specific (Beerling, 2005; Haworth et al., 2010; Jordan, 2011; Royer

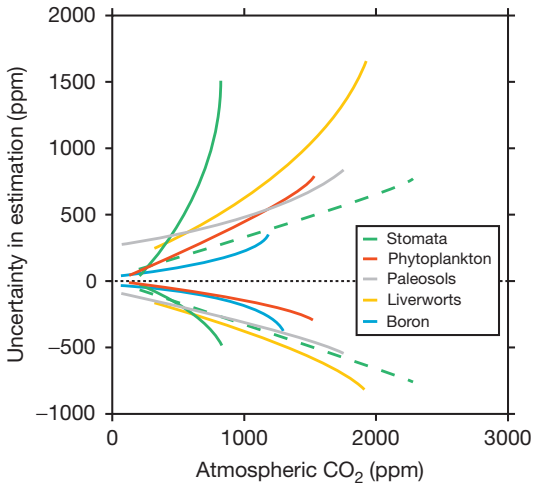

Figure 3 Error analysis for atmospheric CO_2 proxies. Curves are regression fits (CO_2 vs. associated error) of the data presented in **Figure 4**. Positive and negative errors are computed separately. Dashed green lines represent data based on the stomatal ratio proxy.

et al., 2001a). This means that measurements from fossil species should be calibrated to the same extant species. An alternative approach is to compare closely related (but not identical) species; the ratio of the two stomatal measurements is then directly related to CO_2 (McElwain and Chaloner, 1995). The errors associated with this stomatal ratio approach are considerably smaller (green dashed lines in **Figure 3**). But because a stomatal–CO_2 relationship is assumed, not calculated, the CO_2 estimates are semiquantitative, including the associated errors.

A superior alternative is to reconstruct CO_2 from stomatal dimensions and gas exchange considerations alone (Grein et al., 2011). This approach retains sensitivity even at high CO_2 (e.g., standard deviation for an estimate of 2000 ppm is ~200 ppm) and does not require an extant calibration between CO_2 and stomatal index, opening up much more of the paleobotanical record (i.e., species that are extinct today). However, as with the traditional approaches, it requires some uniformitarian assumptions, specifically about photosynthetic and conductance parameters.

6.11.3.2 CO_2: Phytoplankton and Liverworts

In contrast to stomata-bearing plants, most phytoplankton cannot actively control the throughput of CO_2 through their cells. If the concentration of CO_2 rises in the surrounding water, then more CO_2 will pass through their cells. Because photosynthesis fractionates against the heavy isotope ^{13}C (Degens et al., 1968), the carbon isotopic fractionation between CO_2 in ambient seawater and photosynthate, $\Delta_{sea\text{-}photo}$ ($[\delta^{13}C_{sea}-\delta^{13}C_{photo}]/[1+\delta^{13}C_{photo}/1000]$), increases in a high-$CO_2$ environment. This is because the phytoplankton–CO_2 system is more open in a Rayleigh fractionation context. At low CO_2, with a correspondingly low-CO_2 throughput, more ^{13}C is incorporated into photosynthate and $\Delta_{sea\text{-}photo}$ declines (Popp et al., 1989).

The $\delta^{13}C$ and $\delta^{18}O$ of marine carbonate can be used to reconstruct $\delta^{13}C_{sea}$. By coupling isotopic measurements of carbonates with coexisting organic matter ($\delta^{13}C_{photo}$), atmospheric CO_2 can be reconstructed. Many studies use the $\delta^{13}C$ of bulk organic matter as a proxy for $\delta^{13}C_{photo}$ (Arthur et al., 1985; Cramer and Saltzman, 2007; Freeman and Hayes, 1992; Hollander and McKenzie, 1991; Kienast et al., 2001; Kump et al., 1999; Popp et al., 1989; Rothman, 2002; Sarkar et al., 2003; Young et al., 2010). However, even in deep-sea settings, marine nonphotosynthetic and terrestrial organic matter are present in bulk samples (Hayes et al., 1989; Pagani et al., 2000). Also, vital effects related to active HCO_3^- transport (Hinga et al., 1994), growth rate (Fry and Wainwright, 1991), and cell volume/surface area (Popp et al., 1998) can impact $\Delta_{sea\text{-}photo}$. As a result, most studies no longer measure bulk $\delta^{13}C$ but instead, a subset of biomarkers that today are found in a limited number of species. Jasper and Hayes (1990) pioneered the use of C_{37} diunsaturated alkenones, which today are produced mostly by two closely related species of haptophytic algae (Conte et al., 1994). The influence of cell geometry can be calibrated with the appropriate extant taxa (Henderiks and Pagani, 2007) and applied to fossils (Henderiks and Pagani, 2007, 2008), although the fossil measurements are very laborious. The growth rate in fossil algae has proved more difficult to model. Most paleo-CO_2 studies apply the present-day relationship between the growth rate in haptophytic algae and seawater PO_4^{3-} concentration (Bidigare et al., 1997; Pagani, 2002). However, reconstructing paleo-PO_4^{3-} is difficult; most fossil studies use marine sediment cores with strong evidence for oligotrophy and apply PO_4^{3-} concentrations from putatively similar modern seawater (e.g., Pagani et al., 1999b).

Further work is needed to improve the characterization of growth rate in fossil studies, especially considering that some experimental studies find $\Delta_{sea\text{-}photo}$ more strongly impacted by growth rate than by CO_2 concentration (e.g., Benthien et al., 2007). Indeed, the anomalously high CO_2 estimates from the high-latitude sites of Pagani et al. (2005b) may reflect differences in growth rate rather than CO_2. A temporal limitation of the alkenone-based approach is that alkenones are unknown from before the Cretaceous (Farrimond et al., 1986) and remain rare until the middle Eocene. Presently, all alkenone-based CO_2 estimates postdate the early Eocene.

Bryophytes (mosses, liverworts, and hornworts) typically lack stomata in their vegetative tissues. For the purposes of reconstructing CO_2, then, these plants can be considered terrestrial equivalents of phytoplankton. As atmospheric CO_2 rises, the $\delta^{13}C$ of the plant tissue declines, reflecting a more open Rayleigh fractionation system, and vice versa when CO_2 drops. White and colleagues pioneered this proxy, reconstructing Holocene CO_2 from *Sphagnum* moss bogs (Figge and White, 1995; White et al., 1994). As with phytoplankton, an additional control on the $\delta^{13}C$ of bryophytes is growth rate, which is strongly controlled by water content (Price et al., 1997; Rice and Giles, 1996). Fletcher et al. (2005) demonstrated that liverworts have much more stable water contents than most mosses and, thus, are the best candidates for paleo-CO_2 estimation. Fletcher et al. (2006) developed a process-based model for liverwort photosynthesis that calculates atmospheric CO_2 from $\delta^{13}C_{photo}$, $\delta^{13}C_{air}$, temperature, O_2 concentration, irradiance, and a suite of physiological parameters. This proxy is quite young; as more groups use the method, improvements will no doubt come, especially with respect to modeling the physiological parameters.

6.11.3.3 CO_2: Paleosols (Calcite and Goethite)

In arid and semiarid climates, calcite commonly precipitates in soils (Royer, 1999). For soils with noncarbonate parent material and little diagenetic or groundwater influence (Quast et al., 2006), the carbon has two sources: biological respiration within the soil and diffusion of atmospheric CO_2 into the soil. Because the $\delta^{13}C$ of these sources is distinct, an isotopic mass balance can be constructed to calculate atmospheric CO_2 concentration (Cerling, 1984, 1991, 1999):

$$CO_{2[atm]} = S(z)\frac{\delta_s - 1.0044\delta_\phi - 4.4}{\delta_a - \delta_s} \quad [6]$$

where $S(z)$ is the concentration of soil-respired CO_2 and δ_s, δ_ϕ, and δ_a are the $\delta^{13}C$ of soil CO_2 (inferred from soil calcite), soil-respired CO_2 (inferred from organic matter), and atmospheric CO_2 (inferred from coeval shallow marine carbonate). Because carbonate-bearing soils often have little preserved organic matter, atmospheric $\delta^{13}C$ records (e.g., from shallow marine

carbonates) are sometimes used as a proxy (e.g., Ekart et al., 1999), but such an approach is fraught with uncertainty (Beerling and Royer, 2002). Even when the $\delta^{13}C$ of coexisting organic matter can be measured, care must be taken to account for isotopic fractionation during microbial decomposition (Bowen and Beerling, 2004; Wynn, 2007).

Estimating the concentration of soil-respired CO_2 ($S(z)$) is difficult. Older studies typically assumed values of ~5000 ppm based on annually integrated measurements in present-day soils (e.g., Brook et al., 1983). However, Breecker et al. (2009) demonstrated that calcite precipitation is thermodynamically favorable only during the warmer and drier parts of the year. During these times, $S(z)$ is low (usually <2000 ppm). Because atmospheric CO_2 estimates scale directly with $S(z)$, many published estimates may be too high by over a factor of 2 (see also Schroeder et al., 2006). Recognition of this overestimation has been critical for improving paleo-CO_2 records, but the application of a single, revised $S(z)$ (Breecker et al., 2010) ignores the full range of possible $S(z)$. Future work will be directed toward developing more refined indicators of $S(z)$ (Retallack, 2009b).

An analogous atmospheric CO_2 proxy is based on trace carbonate in goethite ($Fe(CO_3)OH$) (Feng and Yapp, 2009; Tabor and Yapp, 2005; Tabor et al., 2004; Yapp, 2004; Yapp and Poths, 1992, 1996). As with the calcite-based proxy, the $\delta^{13}C$ of the carbonate and coexisting organic matter is inputted into a two-end-member mixing model. Critically, the concentration of the trace carbonate scales with the concentration of soil CO_2 (Yapp, 1987; Yapp and Poths, 1991). Thus, in contrast to the calcite method, the concentration of soil-respired CO_2 ($S(z)$) can be computed directly. However, molecular dynamic simulations and quantum chemistry calculations demonstrate that carbonate in goethite is incorporated through two pathways, each with its own carbon isotope fractionation factor (Rustad and Zarzycki, 2008). The standard goethite paleo-CO_2 model assumes a constant fractionation factor and thus needs revision in light of these new results. Changes in soil moisture content and the residence time of soil carbon can also affect CO_2 estimates (Gulbranson et al., 2011).

6.11.3.4 CO_2: Boron ($\delta^{11}B$ and B/Ca)

The relative proportions of the two major boron species in the ocean, $B(OH)_3$ and $B(OH)_4^-$, vary with pH. Because the boron isotopic composition ($\delta^{11}B$) of these two species differs, the $\delta^{11}B$ of marine carbonate is a proxy for seawater pH (Hemming and Hanson, 1992; Palmer et al., 1998; Sanyal et al., 1995, 1996; Spivack et al., 1993; Vengosh et al., 1991). With assumptions about the total alkalinity or dissolved inorganic carbon (DIC) concentration of ancient seawater, atmospheric CO_2 can be inferred from pH (Hönisch and Hemming, 2005; Hönisch et al., 2009; Pearson and Palmer, 1999, 2000; Pearson et al., 2009).

Several critical objections have been raised about this CO_2 method. First, the fractionation factor between $B(OH)_3$ and $B(OH)_4^-$ used by earlier studies (Hönisch and Hemming, 2005; Pearson and Palmer, 1999, 2000) is incorrect (Klochko et al., 2006; Liu and Tossell, 2005; Pagani et al., 2005a; Rustad et al., 2010; Zeebe, 2005). Also, the $\delta^{11}B$ in biologically produced carbonate is usually offset from the theoretical fractionation, and this offset is generally species-specific (e.g., Blamart et al., 2007; Hönisch et al., 2003; Sanyal et al., 1996; Zeebe et al., 2003). At minimum, fossil studies should be calibrated to the same extant species. The boron proxy assumes that only $B(OH)_4^-$ is incorporated into carbonate, but Klochko et al. (2009) determined that $B(OH)_3$ may be active too, and the proportionality of uptake between the two species is pH-dependent; this behavior may explain some of the reported 'vital effects' and further complicates the proxy. Early CO_2 reconstructions assumed constant alkalinity (Pearson and Palmer, 1999), but this is not realistic (Caldeira et al., 1999). More recent reconstructions have used increasingly sophisticated models for alkalinity and DIC (Demicco et al., 2003; Pearson et al., 2009; Roberts and Tripati, 2009; Tyrrell and Zeebe, 2004). Knowledge of the $\delta^{11}B$ of seawater is also needed for pH reconstructions, but quantifying its evolution is difficult (Lemarchand et al., 2000, 2002; Simon et al., 2006). Diagenesis may also impact the $\delta^{11}B$ of carbonate (Hönisch and Hemming, 2004; Spivack and You, 1997; Wara et al., 2003). The impact of diagenesis is particularly worrisome in light of the recognition that carbonate considered pristine using traditional screening protocols may in reality be highly altered isotopically (Pearson et al., 2001). A final roadblock for the boron proxy is that methodological differences have led to interlab differences in $\delta^{11}B$ measurements that exceed the stated precision by eightfold (Foster et al., 2006). A new method based on MC-ICPMS may resolve this precision problem, but further interlab testing is needed (Foster, 2008; Ni et al., 2010).

The CO_2 reconstructions of Pearson and Palmer (1999, 2000) should be considered suspect due to the use of an incorrect fractionation factor, the strong possibility of diagenesis, and the primitive modeling of alkalinity and seawater $\delta^{11}B$. Newer CO_2 reconstructions have made progress on all these fronts (Pearson et al., 2009; Seki et al., 2010), but more work is needed to understand the long-term controls of seawater $\delta^{11}B$ and the species-specific nature of the pH responses. For example, the seawater $\delta^{11}B$ record of Paris et al. (2010) suggests that most pre-Pleistocene CO_2 estimates require substantial downward revision.

Recently, the B/Ca ratio in marine carbonate has been proposed as a proxy for pH and atmospheric CO_2 (Yu et al., 2007). If $B(OH)_4^-$ is the only boron species incorporated into carbonate and its concentration is controlled in part by pH, then the B/Ca ratio in carbonate should reflect pH. This proxy is highly related to the $\delta^{11}B$ proxy, and as such, many of the concerns already outlined are pertinent here (Foster, 2008; Ni et al., 2007; Yu et al., 2007, 2010). Additionally, Allen et al. (2011) report that CO_3^{2-} may be more important than pH in controlling B/Ca and that B/Ca covaries with seawater B concentration and salinity. The controls over boron uptake in shells clearly warrant further study.

6.11.3.5 CO_2: Nahcolite

Nahcolite is a rare sodium carbonate mineral ($NaHCO_3$). Equilibrium experiments demonstrate that in the nahcolite–trona–natron system, nahcolite only precipitates at high CO_2 (>1330 ppm; >1125 ppm if coprecipitated with halite) (Eugster, 1966). The presence of nahcolite may therefore establish a minimum level of atmospheric CO_2. Key assumptions

with this proxy are that the nahcolite precipitates at the air–water interface and that in situ generation of biologically respired CO_2 is minimal (Lowenstein and Demicco, 2006). Application of the proxy is limited because nahcolite is rare: the only geologic deposits are from the Eocene. Nevertheless, the classic nahcolite deposits from the Green River Formation date to the peak of Cenozoic warmth (early Eocene climatic optimum), suggesting a CO_2–temperature link (Lowenstein and Demicco, 2006). Trona, which precipitates at lower CO_2, is also found in coeval Green River deposits, but it lacks primary sedimentary textures and is interpreted to have formed diagenetically at higher temperatures where it is stable. Importantly, new equilibrium experiments find that nahcolite can precipitate at lower CO_2 (Jagniecki et al., 2010), suggesting a downward revision of CO_2 estimates from >1330 ppm to >∼1000 ppm.

Table 1 Sources of CO_2 data presented in **Figures 4–7**

CO_2 proxy	*Sources*
Stomata	van der Burgh et al. (1993); Kürschner et al. (1996, 2001, 2008); Beerling et al. (1998, 2002a); McElwain (1998); McElwain et al. (1999, 2005); Chen et al. (2001); Royer et al. (2001b); Beerling (2002); Beerling and Royer (2002); Greenwood et al. (2003); Roth-Nebelsick and Konrad (2003); Royer (2003); Haworth et al. (2005); Sun et al. (2007); Passalia (2009); Quan et al. (2009); Retallack (2009a); Yan et al. (2009); Barclay et al. (2010); Bonis et al. (2010); Smith et al. (2010); Doria et al. (2011); Steinthorsdottir et al. (2011); Stults et al. (2011); Grein et al. (2011); Wan et al. (2011)
Phytoplankton	Pagani et al. (1999a,b, 2005b, 2011); Seki et al. (2010)
Liverworts	Fletcher et al. (2008)
Paleosol carbonate	Suchecki et al. (1988); Platt (1989); Cerling (1991, 1992); Koch et al. (1992); Muchez et al. (1993); Sinha and Stott (1994); Andrews et al. (1995); Mora et al. (1996); Ekart et al. (1999); Lee (1999); Lee and Hisada (1999); Driese et al. (2000); Cox et al. (2001); Royer et al. (2001b); Tanner et al. (2001); Nordt et al. (2002, 2003); Robinson et al. (2002); Tabor et al. (2004); Ghosh et al. (2005); Prochnow et al. (2006); Sandler (2006); Montañez et al. (2007); Cleveland et al. (2008); Leier et al. (2009); Retallack (2009b); Schaller et al. (2011)
Boron ($\delta^{11}B$)	Pearson et al. (2009); Seki et al. (2010)
Boron (B/Ca)	Tripati et al. (2009)
Nahcolite	Lowenstein and Demicco (2006)

Notes: All dates are calibrated to the timescale of Gradstein et al. (2004). Many individual CO_2 estimates are based on multiple measurements of the same material; consult sources for details. The boron-based estimates of Pearson and Palmer (2000) are omitted owing to their lack of reliability (**Section 6.11.3.4**). No goethite-based estimates are presented owing to the poor knowledge of some of the isotopic fractionation factors (**Section 6.11.3.3**). Liverwort estimates have been updated using the atmospheric $\delta^{13}C$ record of Tipple et al. (2010). Paleosol carbonate estimates have been recalculated assuming a soil respiration concentration of 2000 ppm (Breecker et al., 2009). Stomatal ratio estimates have been recalculated following the procedure of Beerling and Royer (2002). For Retallack (2009a), which emend Retallack (2001, 2002), only estimates based on >4 cuticles (Royer, 2003) and from the genus *Ginkgo* (Vörding and Kerp, 2008) are included; for fossil species other than *Ginkgo adiantoides*, the stomatal ratio method was applied. The high-resolution record of Doria et al. (2011) has been combined into a single estimate. Some Permo–Carboniferous data of Ekart et al. (1999) have been updated by Tabor et al. (2004) and Montañez et al. (2007). Beerling et al. (2009) emend the estimates of Royer et al. (2001b), Beerling et al. (2002a), Royer (2003), and Kürschner et al. (2008). Ghosh et al. (2005) emend the estimates of Ghosh et al. (1995, 2001), and Henderiks and Pagani (2008) emend the estimates of Pagani et al. (1999a,b, 2005b). Southern high-latitude sites from Pagani et al. (2005b, 2011) are excluded; see Pagani et al. (2011) for justification. Estimates from Pagani et al. (2011) follow their Figure 4.

6.11.3.6 Estimates of Phanerozoic CO_2 from Proxies

A Phanerozoic CO_2 history from proxies is presented in **Figure 4(a)**. Two points are worth noting: First, although there is some scatter at any given time interval, the variability

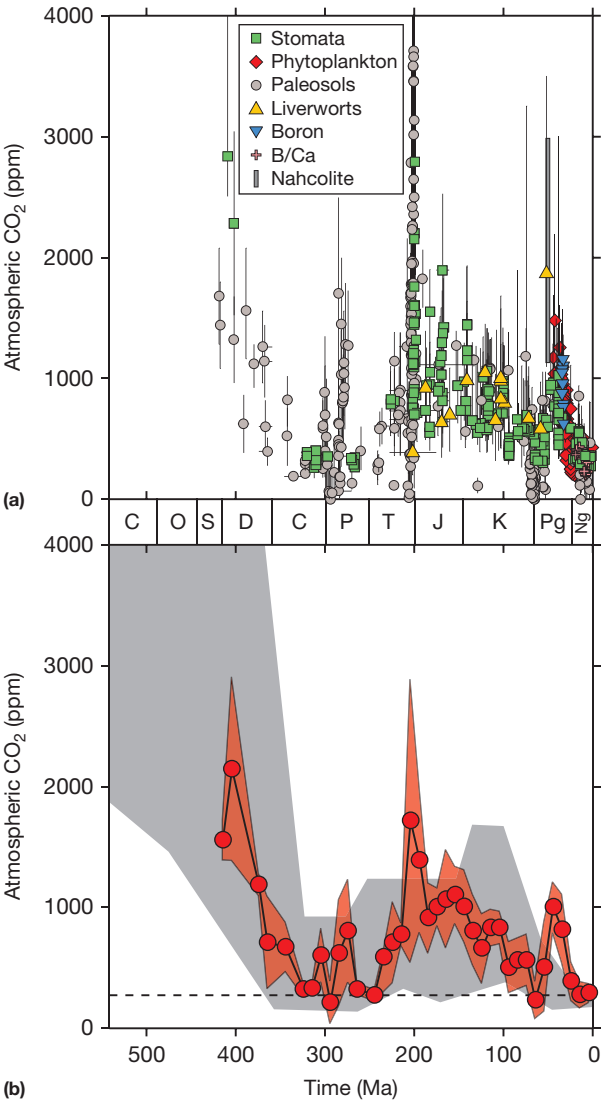

Figure 4 Phanerozoic history of atmospheric CO_2 from proxies. (a) Individual CO_2 estimates, coded by proxy type ($n=761$). See **Table 1** for data sources. Some estimates from Schaller et al. (2011) near the T/J boundary exceed 4000 ppm and are not visible. (b) CO_2 estimates averaged into 10 My bins (red circles). Bins represented by single estimates are excluded; red band captures $\pm1\sigma$ of the binned data set. The 10 My time step allows a cleaner comparison to the GEOCARB output (gray band, from **Figure 2(a)**), which has the same time step.

is typically less than twofold. Second, there is a broad agreement among methods (see also **Figures 5–7**). This contrasts with earlier compilations that found much higher variability (e.g., >3000 ppm for the early Paleogene; Royer, 2003). Much of the discrepancy has been resolved through the downward revision of paleosol estimates (Breecker et al., 2010), the upward revision of stomatal estimates (Beerling et al., 2009), and the exclusion of suspect boron estimates (see **Section 6.11.3.4**). An example of reconciliation is drawn from Royer et al. (2001b), who reported pairs of CO_2 estimates from the paleosol and stomatal methods. Here, the large discrepancies between methods largely disappear after incorporating the revisions of Beerling et al. (2009) and Breecker et al. (2010) (**Figure 5**).

Proxy estimates broadly match the independently derived model estimates (**Figure 4(b)**). Both show a 'double hump' pattern of CO_2, with elevated CO_2 during the early Paleozoic and mid-Mesozoic, and a possible secondary 'hump' during the early Cenozoic. Together, they bolster confidence that the long-term (10 My time step) patterns of atmospheric CO_2 are well described.

6.11.3.7 O_2 Proxies

Proxy development for atmospheric O_2 lags far behind that for CO_2. Combustion experiments suggest a minimum oxygen content of 15% to support wildfire (Belcher and McElwain, 2008; Belcher et al., 2010). Charcoal is a product of wildfire and is present in the geologic record, with few exceptions, throughout the last 420 My when vascular plants were common (Chaloner, 1989; Cope and Chaloner, 1980; Glasspool et al., 2004; Scott, 2000). This suggests that atmospheric O_2 exceeded 15% for much of the Phanerozoic, a result in accord with geochemical calculations (**Figure 2(b)**).

Upper O_2 limits are less constrained by proxies. Early combustion experiments suggested runaway wildfires at levels above ~25%, but newer experiments do not support this claim (Berner et al., 2003; Wildman et al., 2004b). During the Carboniferous and Permian, when geochemical models predict O_2 levels up to 35% (**Figure 2(b)**), charcoal is more abundant than at most other times during the Phanerozoic (Robinson, 1991; Scott, 2000). Indeed, the fraction of charcoal macerals in coal quantitatively tracks the rise of O_2 into the Carboniferous as predicted from geochemical models (Diessel, 2010; Glasspool and Scott, 2010; Scott and Glasspool, 2006), providing strong, independent support for an O_2 spike at that time.

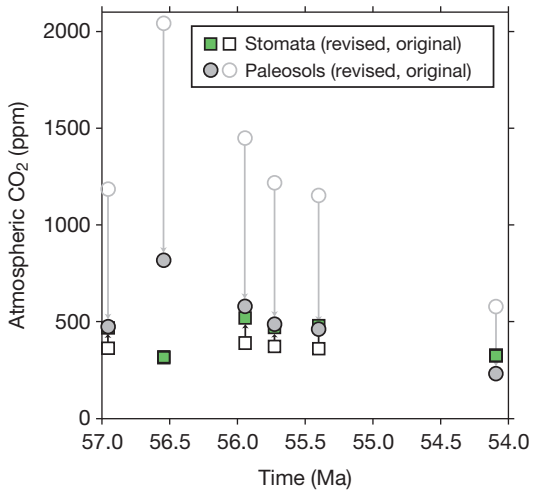

Figure 5 Atmospheric CO_2 estimates from the Bighorn Basin, Wyoming. Each CO_2 pair corresponds to stratigraphically equivalent beds (within 15 m or ~30 ky). Original estimates (open symbols) are from Royer et al. (2001b). Stomatal estimates have been revised following the error propagation method of Beerling et al. (2009). Paleosol carbonate estimates have been recalculated assuming a soil respiration concentration of 2000 ppm (Breecker et al., 2009).

6.11.4 Impacts of CO_2 and O_2 on Climate and Life

6.11.4.1 CO_2–Temperature Coupling

A rich body of evidence supports a strong link between atmospheric CO_2 and temperature for much of the Phanerozoic (e.g., Berner, 1991; Bijl et al., 2010; Came et al., 2007; Crowley and Berner, 2001; Montañez et al., 2007; Royer, 2006; Vaughan, 2007). In particular, the two most long-lived Phanerozoic glaciations during the Permo–Carboniferous

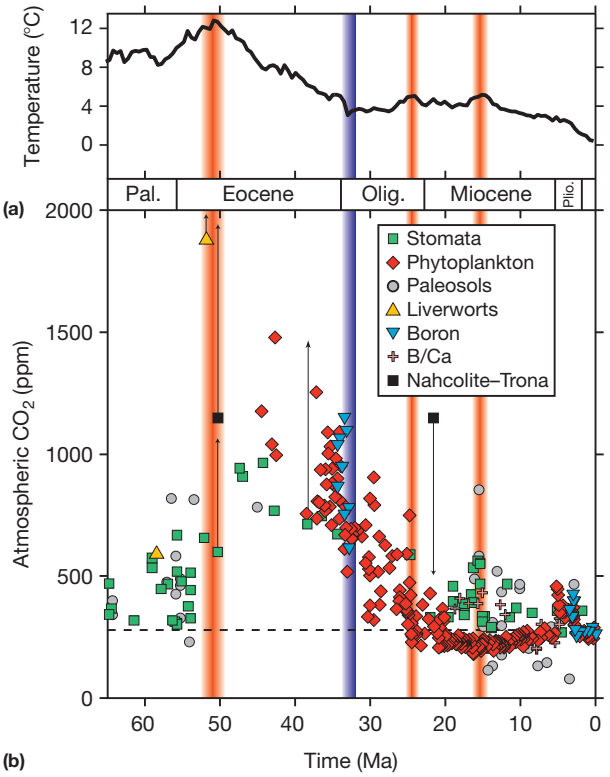

Figure 6 CO_2–temperature coupling during the Cenozoic. (a) Global-mean surface temperature, as calculated from the benthic $\delta^{18}O$ compilation of Zachos et al. (2008) and following the protocol of Hansen et al. (2008). Temperature is expressed relative to the preindustrial. (b) Individual CO_2 estimates, coded by proxy type. See **Table 1** for data sources. Estimates with arrows are unbounded. Red bands correspond to pulses in global warmth; the blue band corresponds to the rapid cooling coincident with the inception of Antarctic ice growth (Zachos et al., 2008). Dashed line represents preindustrial CO_2 concentration (280 ppm). This figure is updated from Beerling and Royer (2011).

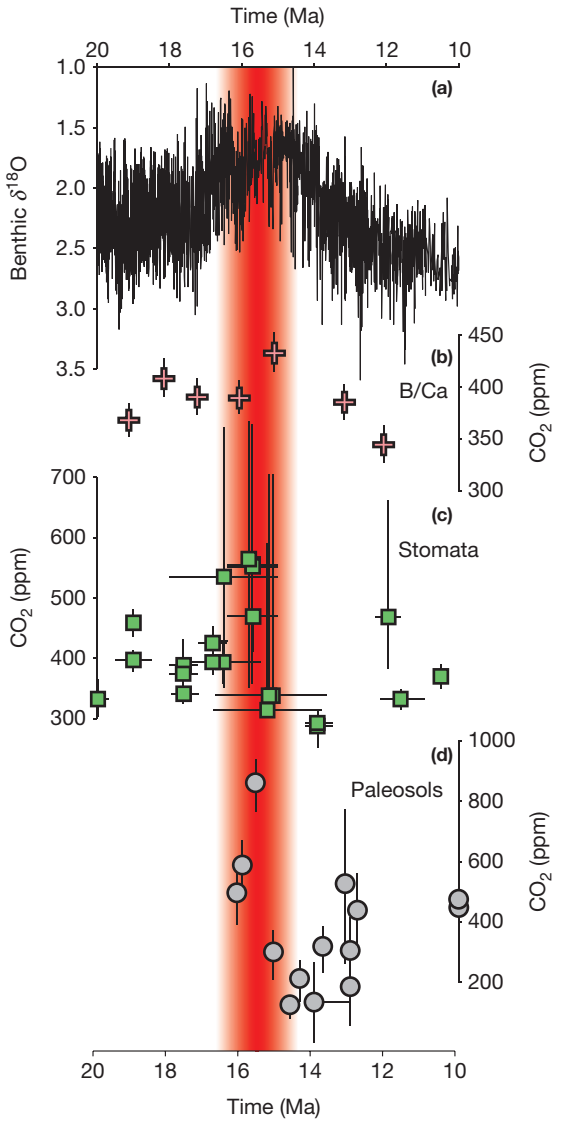

Figure 7 Benthic $\delta^{18}O$ and atmospheric CO_2 records for the Middle Miocene. Benthic record is from Zachos et al. (2008). CO_2 estimates are coded by proxy type (see **Table 1** for data sources). The red band demarcates the Middle Miocene climatic optimum.

(~340–260 Ma) and late Cenozoic (35–0 Ma) correspond to low (<500 ppm) levels of CO_2 (Crowley and Berner, 2001) (**Figure 4**). Even short-term events, such as the 'cool snaps' during the Mesozoic, often are linked to temperature (Royer, 2006). No CO_2 proxy estimates are currently available for the end-Ordovician glaciation, but models predict a minimum of 1500 ppm (**Figure 4**). This level of CO_2 may seem at odds with a glacial climate, but because solar luminosity was ~4% lower than the present, the CO_2 threshold for nucleating ice sheets was likely ~2000–4000 ppm (Crowley and Baum, 1991, 1995; Gibbs et al., 1997, 2000; Herrmann et al., 2003, 2004; Kump et al., 1999; Poussart et al., 1999). A similar scenario exists for the putative glacial interval during the late Cambrian (Runkel et al., 2010).

There is a strong CO_2–temperature coupling during the Cenozoic (**Figure 6**) (see also Beerling and Royer, 2011). CO_2 rose during the Paleocene, peaking at 1000+ ppm during the early Eocene, corresponding with the peak of Cenozoic warmth. CO_2 then fell during the Eocene, tracking cooling global temperatures, before plummeting at the Eocene–Oligocene boundary, a time marked by the onset of glaciation on Antarctica. Two CO_2 peaks during the late Oligocene and Middle Miocene coincide with well-known warm periods (**Figures 6** and **7**). Despite this apparent coupling, several inconsistencies remain: First, the phytoplankton method does not pick up the Middle Miocene CO_2 spike, but three other methods do (stomata, paleosols, and B/Ca) (**Figure 7**). Second, Paleocene CO_2 levels are low – similar to Oligocene values – despite clear evidence that temperatures were warmer during the Paleocene. Either climate sensitivity to CO_2 was high during the Paleocene or the CO_2 data are in error.

For some parts of the Phanerozoic, CO_2 and temperature records are sufficiently robust (numerous, convergent estimates) to compute climate sensitivity. During the Pleistocene, climate sensitivity was ~6 °C per CO_2 doubling (Hansen et al., 2008). Critically, this is approximately double the value typically calculated from global climate models and historical records from the last 1000 years (~3 °C) (IPCC, 2007). The discrepancy is due to models and historical data not capturing long-term processes, such as the waxing and waning of continental ice sheets (Hansen et al., 2008). For geological studies, the longer-term response, sometimes called Earth system sensitivity (Lunt et al., 2010), is more appropriate. Although the computation of Earth system sensitivity is a frontier area, a pattern is emerging of 6+ °C sensitivity during glacial times and 3–6 °C during nonglacial times (Hansen et al., 2008; Lunt et al., 2010; Pagani et al., 2010; Park and Royer, 2011; Royer, 2010; Royer et al., 2007; see also **Chapter 6.13**). The amplification during glacial times is probably due to a stronger ice–albedo climate feedback, but even during nonglacial times, Earth system sensitivity is higher than what is calculated for the present day. The underlying reason for this is unclear but points to the presence of presently unknown climate feedbacks (see **Chapter 6.13**). Identifying these feedbacks will greatly expand the fundamental understanding of the ice-free Earth system, for example, the long-standing enigma of flatter latitudinal temperature gradients during ice-free times (e.g., Ballantyne et al., 2010; Bijl et al., 2009; Hollis et al., 2009).

6.11.4.2 Linking Trees to Giant Insects During the Carboniferous and Permian

One elegant case study that highlights the two-way interplay between evolution and geochemical cycling is the evolution of forests during the Devonian facilitating the evolution of giant insects during the Carboniferous and Permian. As discussed earlier (**Section 6.11.2.2.1**), plants enhance the chemical weathering rate of silicate minerals, a process that shuttles carbon from the atmosphere to the carbonate rock reservoir (**Figure 1**). As a result, the evolution of forests during the Devonian probably led to a global increase in weathering rate, which was brought back into balance through the attendant CO_2 drawdown and associated cooling (Berner, 1997, 1998). The evolution of forests also significantly increased the amount of carbon stored on land, principally in the form of wood and soil organic matter. Further, components of wood

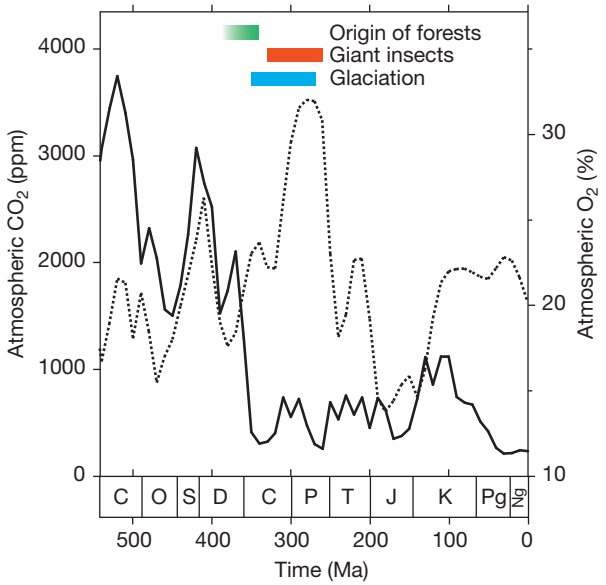

Figure 8 Phanerozoic history of atmospheric CO_2 and O_2 and key evolutionary and climatic events during the Paleozoic. CO_2 and O_2 histories are taken from **Figure 2**. Timing for the evolution of forests is taken from Willis and McElwain (2002), insect gigantism from Berner et al. (2007), and glaciation from Isbell et al. (2003).

like lignin, which did not exist in abundance before the rise of woody plants, are highly resistant to decomposition. Taken together, both the size and chemical composition of this new reservoir of reduced carbon increased the likelihood for organic matter burial (e.g., Robinson, 1990). The geologic record strongly supports this scenario: the Phanerozoic peak in organic matter burial occurs during the Carboniferous and Permian (Berner, 2003). The massive coal deposits from this interval are the most obvious manifestation of this burial.

The evolution of forests and its attendant increase in organic matter burial would have two first-order impacts on atmospheric composition (**Figure 1**): a drop in CO_2 and a rise in O_2 (**Figure 8**). The CO_2 drop was likely a critical driver for the Permo–Carboniferous glaciation, the most intense and long-lived glaciation during the Phanerozoic (**Section 6.11.4.1**). Equally important, the O_2 rise probably profoundly impacted evolution. A general link between oxygen and evolution is well established (Berner et al., 2007; Budyko et al., 1987; McAlester, 1970). Animals, in particular, are sensitive owing to their intensive oxygen needs (**Chapter 6.10**). In the fossil record, the most pronounced interval of insect gigantism coincides with the Permo–Carboniferous O_2 spike (**Figure 8**) (Berner et al., 2003, 2007; Graham et al., 1995). Insects were up to ten times larger than similar extant groups, including dragonflies with 70 cm wingspans and 2 m long millipedes (Graham et al., 1995; Harrison et al., 2010). All insects rely on tracheal networks for respiration, whose volumetric contribution to body volume may place an upper limit on body size that scales with atmospheric O_2 concentration (Kaiser et al., 2007; VandenBrooks et al., 2012). A growing body of experimental evidence links atmospheric O_2 content to body size and metabolism in insects (see summaries in Berner et al., 2003; Harrison et al., 2010). If atmospheric oxygen levels reached 35%, then total atmospheric pressure would have increased by 25% relative to the Devonian (Berner, 2006b). For flying insects, this may have also relaxed upper limits on body size (Dudley, 2000).

Acknowledgments

The author thanks Bob Berner for his long-time collaboration and for comments on the manuscript. The author also thanks K. Klochko, T. Lowenstein, and J. VandenBrooks for helpful discussions. The author is grateful to the Mellon Foundation for supporting a College of the Environment fellowship.

References

Allen KA, Hönisch B, Eggins SM, Yu J, Spero HJ, and Elderfield H (2011) Controls on boron incorporation in cultured tests of the planktic foraminifera *Orbulina universa*. *Earth and Planetary Science Letters* 309: 291–301.

Andrews J and Schlesinger W (2001) Soil CO_2 dynamics, acidification, and chemical weathering in a temperate forest with experimental CO_2 enrichment. *Global Biogeochemical Cycles* 15: 149–162.

Andrews JE, Tandon SK, and Dennis PF (1995) Concentration of carbon dioxide in the Late Cretaceous atmosphere. *Journal of the Geological Society of London* 152: 1–3.

Arrhenius S (1896) On the influence of carbonic acid in the air upon the temperature on the ground. *Philosophical Magazine and Journal of Science* 41: 237–275.

Arthur MA, Dean WE, and Claypool GE (1985) Anomalous ^{13}C enrichment in modern marine organic carbon. *Nature* 315: 216–218.

Arvidson RS, Mackenzie FT, and Guidry M (2006) MAGic: A Phanerozoic model for the geochemical cycling of major rock-forming components. *American Journal of Science* 306: 135–190.

Baars C, Jones TH, and Edwards D (2008) Microcosm studies of the role of land plants in elevating soil carbon dioxide and chemical weathering. *Global Biogeochemical Cycles* 22: GB3019. http://dx.doi.org/10.1029/2008GB003228.

Ballantyne AP, Greenwood DR, Sinninghe Damsté JS, Csank AZ, Eberle JJ, and Rybczynski N (2010) Significantly warmer Arctic surface temperatures during the Pliocene indicated by multiple independent proxies. *Geology* 38: 603–606.

Barclay RS, McElwain JC, and Sageman BB (2010) Carbon sequestration activated by a volcanic CO_2 pulse during Ocean Anoxic Event 2. *Nature Geoscience* 3: 205–208.

Beerling DJ (2002) Low atmospheric CO_2 levels during the Permo-Carboniferous glaciation inferred from fossil lycopsids. *Proceedings of the National Academy of Sciences of the United States of America* 99: 12567–12571.

Beerling DJ (2005) Evolutionary responses of land plants to atmospheric CO_2. In: Ehleringer JR, Cerling TE, and Dearing MD (eds.) *A History of Atmospheric CO_2 and Its Effects on Plants, Animals, and Ecosystems*, pp. 114–132. New York: Springer.

Beerling DJ (2007) *The Emerald Planet: How Plants Changed Earth's History*. Oxford: Oxford University Press.

Beerling DJ, Fox A, and Anderson CW (2009) Quantitative uncertainty analyses of ancient atmospheric CO_2 estimates from fossil leaves. *American Journal of Science* 309: 775–787.

Beerling DJ, Lake JA, Berner RA, Hickey LJ, Taylor DW, and Royer DL (2002a) Carbon isotope evidence implying high O_2/CO_2 ratios in the Permo-Carboniferous atmosphere. *Geochimica et Cosmochimica Acta* 66: 3757–3767.

Beerling DJ, Lomax BH, Royer DL, Upchurch GR, and Kump LR (2002b) An atmospheric pCO_2 reconstruction across the Cretaceous-Tertiary boundary from leaf megafossils. *Proceedings of the National Academy of Sciences of the United States of America* 99: 7836–7840.

Beerling DJ, McElwain JC, and Osborne CP (1998) Stomatal responses of the 'living fossil' Ginkgo biloba L. to changes in atmospheric CO_2 concentrations. *Journal of Experimental Botany* 49: 1603–1607.

Beerling DJ and Royer DL (2002) Fossil plants as indicators of the Phanerozoic global carbon cycle. *Annual Review of Earth and Planetary Sciences* 30: 527–556.

Beerling DJ and Royer DL (2011) Convergent Cenozoic CO_2 history. *Nature Geoscience* 4: 418–420.

Belcher CM and McElwain JC (2008) Limits for combustion in low O_2 redefine paleoatmospheric predictions for the Mesozoic. *Science* 321: 1197–1200.

Belcher CM, Yearsley JM, Hadden RM, McElwain JC, and Rein G (2010) Baseline intrinsic flammability of Earth's ecosystems estimated from paleoatmospheric

oxygen over the past 350 million years. *Proceedings of the National Academy of Sciences of the United States of America* 107: 22448–22453.
Benthien A, Zondervan I, Engel A, Hefter J, Terbrüggen A, and Riebesell U (2007) Carbon isotopic fractionation during a mesocosm bloom experiment dominated by *Emiliania huxleyi*: Effects of CO_2 concentration and primary production. *Geochimica et Cosmochimica Acta* 71: 1528–1541.
Bergman NM, Lenton TM, and Watson AJ (2004) COPSE: A new model of biogeochemical cycling over Phanerozoic time. *American Journal of Science* 304: 397–437.
Berner RA (1991) A model for atmospheric CO_2 over Phanerozoic time. *American Journal of Science* 291: 339–376.
Berner RA (1992) Weathering, plants, and the long-term carbon cycle. *Geochimica et Cosmochimica Acta* 56: 3225–3231.
Berner RA (1994) GEOCARB II: A revised model of atmospheric CO_2 over Phanerozoic time. *American Journal of Science* 294: 56–91.
Berner RA (1997) The rise of plants and their effect on weathering and atmospheric CO_2. *Science* 276: 544–546.
Berner RA (1998) The carbon cycle and CO_2 over Phanerozoic time: The role of land plants. *Philosophical Transactions of the Royal Society of London* B 353: 75–82.
Berner RA (2001) Modeling atmospheric O_2 over Phanerozoic time. *Geochimica et Cosmochimica Acta* 65: 685–694.
Berner RA (2003) The long-term carbon cycle, fossil fuels and atmospheric composition. *Nature* 426: 323–326.
Berner RA (2004) *The Phanerozoic Carbon Cycle: CO_2 and O_2*. New York: Oxford University Press.
Berner RA (2005) The carbon and sulfur cycles and atmospheric oxygen from middle Permian to middle Triassic. *Geochimica et Cosmochimica Acta* 69: 3211–3217.
Berner RA (2006a) GEOCARBSULF: A combined model for Phanerozoic atmospheric O_2 and CO_2. *Geochimica et Cosmochimica Acta* 70: 5653–5664.
Berner RA (2006b) Geological nitrogen cycle and atmospheric N_2 over Phanerozoic time. *Geology* 34: 413–416.
Berner RA (2006c) Inclusion of the weathering of volcanic rocks in the GEOCARBSULF model. *American Journal of Science* 306: 295–302.
Berner RA (2008) Addendum to "inclusion of the weathering of volcanic rocks in the GEOCARBSULF model" (R. A. Berner, 2006, v. 306, p. 295–302). *American Journal of Science* 308: 100–103.
Berner RA (2009) Phanerozoic atmospheric oxygen: New results using the GEOCARBSULF model. *American Journal of Science* 309: 603–606.
Berner RA, Beerling DJ, Dudley R, Robinson JM, and Wildman RA (2003) Phanerozoic atmospheric oxygen. *Annual Review of Earth and Planetary Sciences* 31: 105–134.
Berner RA and Canfield D (1989) A new model for atmospheric oxygen over Phanerozoic time. *American Journal of Science* 289: 333–361.
Berner RA and Kothavala Z (2001) GEOCARB III: A revised model of atmospheric CO_2 over Phanerozoic time. *American Journal of Science* 301: 182–204.
Berner RA, Lasaga AC, and Garrels RM (1983) The carbonate-silicate geochemical cycle and its effect on atmospheric carbon dioxide over the past 100 million years. *American Journal of Science* 283: 641–683.
Berner RA and Maasch KA (1996) Chemical weathering and controls on atmospheric O_2 and CO_2: Fundamental principles were enunciated by J.J. Ebelmen in 1845. *Geochimica et Cosmochimica Acta* 60: 1633–1637.
Berner RA, Petsch ST, Lake JA, et al. (2000) Isotope fractionation and atmospheric oxygen: Implications for Phanerozoic O_2 evolution. *Science* 287: 1630–1633.
Berner RA, VandenBrooks JM, and Ward PD (2007) Oxygen and evolution. *Science* 316: 557–558.
Berry JA, Troughton JH, and Björkman O (1972) Effect of oxygen concentration during growth on carbon isotope discrimination in C_3 and C_4 species of *Atriplex*. *Carnegie Institution Year Book* 71: 158–161.
Bidigare RR, Fluegge A, Freeman KH, et al. (1997) Consistent fractionation of ^{13}C in nature and in the laboratory: Growth-rate effects in some haptophyte algae. *Global Biogeochemical Cycles* 11: 279–292.
Bijl PK, Houben AJP, Schouten S, et al. (2010) Transient Middle Eocene atmospheric CO_2 and temperature variations. *Science* 330: 819–821.
Bijl PK, Schouten S, Sluijs A, Reichart G-J, Zachos JC, and Brinkhuis H (2009) Early Palaeogene temperature evolution of the southwest Pacific Ocean. *Nature* 461: 776–779.
Blamart D, Rollion-Bard C, Meibom A, Cuif J-P, Juillet-Leclerc A, and Dauphin Y (2007) Correlation of boron isotopic composition with ultrastructure in the deep-sea coral *Lophelia pertusa*: Implications for biomineralization and paleo-pH. *Geochemistry, Geophysics, Geosystems* 8: Q12001. http://dx.doi.org/10.1029/2007GC001686.
Bolton EW, Berner RA, and Petsch ST (2006) The weathering of sedimentary organic matter as a control on atmospheric O_2: II. Theoretical modeling. *American Journal of Science* 306: 575–615.
Bonis NR, Van Konijnenburg-Van Cittert JHA, and Kürschner WM (2010) Changing CO_2 conditions during the end-Triassic inferred from stomatal frequency analysis on *Lepidopteris ottonis* (Goeppert) Schimper and *Ginkgoites taeniatus* (Braun) Harris. *Palaeogeography, Palaeoclimatology, Palaeoecology* 295: 146–161.
Bowen GJ and Beerling DJ (2004) An integrated model for soil organic carbon and CO_2: Implications for paleosol carbonate pCO_2 paleobarometry. *Global Biogeochemical Cycles* 18: 1026. http://dx.doi.org/10.1029/2003GB002117.
Breecker DO, Sharp ZD, and McFadden LD (2009) Seasonal bias in the formation and stable isotopic composition of pedogenic carbonate in modern soils from central New Mexico, USA. *Geological Society of America Bulletin* 121: 630–640.
Breecker DO, Sharp ZD, and McFadden LD (2010) Atmospheric CO_2 concentrations during ancient greenhouse climates were similar to those predicted for A.D. 2100. *Proceedings of the National Academy of Sciences of the United States of America* 107: 576–580.
Brook GA, Folkoff ME, and Box EO (1983) A world model of soil carbon dioxide. *Earth Surface Landforms* 8: 79–88.
Budyko MI, Ronov AB, and Yanshin AL (1987) History of the Earth's Atmosphere. Berlin: Springer.
Caldeira K, Berner R, Sundquist ET, Pearson PN, and Palmer MR (1999) Seawater pH and atmospheric carbon dioxide. *Science* 286: 2043a.
Came RE, Eiler JM, Veizer J, Azmy K, Brand U, and Weidman CR (2007) Coupling of surface temperatures and atmospheric CO_2 concentrations during the Palaeozoic era. *Nature* 449: 198–201.
Casson S and Gray JE (2008) Influence of environmental factors on stomatal development. *New Phytologist* 178: 9–23.
Cerling T (1984) The stable isotopic composition of modern soil carbonate and its relationship to climate. *Earth and Planetary Science Letters* 71: 229–240.
Cerling TE (1991) Carbon dioxide in the atmosphere: Evidence from Cenozoic and Mesozoic paleosols. *American Journal of Science* 291: 377–400.
Cerling TE (1992) Use of carbon isotopes in paleosols as an indicator of the $P(CO_2)$ of the paleoatmosphere. *Global Biogeochemical Cycles* 6: 307–314.
Cerling TE (1999) Stable carbon isotopes in palaeosol carbonates. *Special Publications of the International Association of Sedimentologists* 27: 43–60.
Chaloner WG (1989) Fossil charcoal as an indicator of paleoatmospheric oxygen level. *Journal of the Geological Society of London* 146: 171–174.
Chamberlin TC (1897) A group of hypotheses bearing on climatic changes. *Journal of Geology* 5: 653–683.
Chamberlin TC (1898) The influence of great epochs of limestone formation upon the constitution of the atmosphere. *Journal of Geology* 6: 609–621.
Chamberlin TC (1899) An attempt to frame a working hypothesis of the cause of glacial periods on an atmospheric basis. *Journal of Geology* 7: 545–584.
Chen L-Q, Li C-S, Chaloner WG, et al. (2001) Assessing the potential for the stomatal characters of extant and fossil *Ginkgo* leaves to signal atmospheric CO_2 change. *American Journal of Botany* 88: 1309–1315.
Cleveland DM, Nordt LC, Dworkin SI, and Atchley SC (2008) Pedogenic carbonate isotopes as evidence for extreme climatic events preceding the Triassic-Jurassic boundary: Implications for the biotic crisis? *Geological Society of America Bulletin* 120: 1408–1415.
Conte MH, Volman JK, and Eglinton G (1994) Lipid biomarkers of the Haptophyta. In: Green JC and Leadbeater BSC (eds.) *The Haptophyte Algae*, pp. 351–377. Oxford: Clarendon Press.
Cope MJ and Chaloner WG (1980) Fossil charcoals as evidence of past atmospheric composition. *Nature* 283: 647–649.
Cox JE, Railsback LB, and Gordon EA (2001) Evidence from Catskill pedogenic carbonates for a rapid Late Devonian decrease in atmospheric carbon dioxide concentrations. *Northeastern Geology and Environmental Sciences* 23: 91–102.
Cramer BD and Saltzman MR (2007) Early Silurian paired $\delta^{13}C_{carb}$ and $\delta^{13}C_{org}$ analyses from the Midcontinent of North America: Implications for paleoceanography and paleoclimate. *Palaeogeography, Palaeoclimatology, Palaeoecology* 256: 195–203.
Crowley TJ and Baum SK (1991) Toward reconciliation of Late Ordovician (440 Ma) glaciation with very high CO2 levels. *Journal of Geophysical Research* 96: 22597–22610.
Crowley TJ and Baum SK (1995) Reconciling Late Ordovician (440 Ma) glaciation with very high (14X) CO_2 levels. *Journal of Geophysical Research* 100: 1093–1101.
Crowley TJ and Berner RA (2001) CO_2 and climate change. *Science* 292: 870–872.
Dallanave E, Tauxe L, Muttoni G, and Rio D (2010) Silicate weathering machine at work: Rock magnetic data from the late Paleocene-early Eocene Cicogna section, Italy. *Geochemistry, Geophysics, Geosystems* 11: Q07008. http://dx.doi.org/10.1029/2010GC003142.
Degens ET, Guillard RRL, Sackett WM, and Hellebust JA (1968) Metabolic fractionation of carbon isotopes in marine plankton: I. Temperature and respiration experiments. *Deep Sea Research* 15: 1–9.

Demicco RV, Lowenstein TK, and Hardie LA (2003) Atmospheric pCO_2 since 60 Ma from records of seawater pH, calcium, and primary carbonate mineralogy. *Geology* 31: 793–796.

Diessel CFK (2010) The stratigraphic distribution of inertinite. *International Journal of Coal Geology* 81: 251–268.

Donnadieu Y, Goddéris Y, and Bouttes N (2009) Exploring the climatic impact of the continental vegetation on the Mesozoic atmospheric CO_2 and climate history. *Climate of the Past* 5: 85–96.

Donnadieu Y, Goddéris Y, Pierrehumbert RT, Dromart G, Fluteau F, and Jacob R (2006a) A GEOCLIM simulation of climatic and biogeochemical consequences of Pangea breakup. *Geochemistry, Geophysics, Geosystems* 7: Q11019. http://dx.doi.org/10.1029/2006GC001278.

Donnadieu Y, Pierrehumbert R, Jacob R, and Fluteau F (2006b) Modelling the primary control of paleogeography on Cretaceous climate. *Earth and Planetary Science Letters* 248: 426–437.

Doria G, Royer DL, Wolfe AP, Fox A, Westgate JA, and Beerling DJ (2011) Declining atmospheric CO_2 during the late Middle Eocene climate transition. *American Journal of Science* 311: 63–75.

Driese SG, Mora CI, and Elick JM (2000) The paleosol record of increasing plant diversity and depth of rooting and changes in atmospheric pCO_2 in the Siluro-Devonian. In: Gastaldo RA and DiMichele WA (eds.) *Phanerozoic Terrestrial Ecosystems,* pp. 47–61. Paleontological Society Special Papers 6.

Dudley R (2000) *The Biomechanics of Insect Flight: Form, Function, Evolution*. Princeton, NJ: Princeton University Press.

Ebelmen JJ (1845) Sur les produits de la décomposition des especes minérales de la famille des silicates. *Annales des Mines* 7: 3–66.

Ekart DD, Cerling TE, Montañez IP, and Tabor NJ (1999) A 400 million year carbon isotope record of pedogenic carbonate: Implications for paleoatmospheric carbon dioxide. *American Journal of Science* 299: 805–827.

Eugster HP (1966) Sodium carbonate-bicarbonate minerals as indicators of P_{CO_2}. *Journal of Geophysical Research* 71: 3369–3377.

Falkowski PG, Katz ME, Milligan AJ, et al. (2005) The rise of oxygen over the past 205 million years and the evolution of large placental mammals. *Science* 309: 2202–2204.

Farrimond P, Eglinton G, and Brassell SC (1986) Alkenones in Cretaceous black shales, Blake-Bahama Basin, western North Atlantic. *Organic Geochemistry* 10: 897–903.

Feng W and Yapp CJ (2009) Paleoenvironmental implications of concentration and $^{13}C/^{12}C$ ratios of $Fe(CO_3)OH$ in goethite from a mid-latitude Cenomanian laterite in southwestern Minnesota. *Geochimica et Cosmochimica Acta* 73: 2559–2580.

Figge RA and White JWC (1995) High-resolution Holocene and late glacial atmospheric CO_2 record: Variability tied to changes in thermohaline circulation. *Global Biogeochemical Cycles* 9: 391–403.

Fletcher BJ, Beerling DJ, Royer DL, and Brentnall SJ (2005) Fossil bryophytes as recorders of ancient CO_2 levels: Experimental evidence and a Cretaceous case study. *Global Biogeochemical Cycles* 19: GB3012. http://dx.doi.org/10.1029/2005GB002495.

Fletcher BJ, Brentnall SJ, Anderson CW, Berner RA, and Beerling DJ (2008) Atmospheric carbon dioxide linked with Mesozoic and early Cenozoic climate change. *Nature Geoscience* 1: 43–48.

Fletcher BJ, Brentnall SJ, Quick WP, and Beerling DJ (2006) BRYOCARB: A process-based model of thallose liverwort carbon isotope fractionation in response to CO_2, O_2, light and temperature. *Geochimica et Cosmochimica Acta* 70: 5676–5691.

Foster GL (2008) Seawater pH, CO_2 and $[CO_3^{2-}]$ variations in the Caribbean Sea over the last 130 kyr: A boron isotope and B/Ca study of planktonic foraminifera. *Earth and Planetary Science Letters* 271: 254–266.

Foster GL, Ni Y, Haley B, and Elliott T (2006) Accurate and precise isotopic measurement of sub-nanogram sized samples of foraminiferal hosted boron by total evaporation NTIMS. *Chemical Geology* 230: 161–174.

Freeman KH and Hayes JM (1992) Fractionation of carbon isotopes by phytoplankton and estimates of ancient CO_2 levels. *Global Biogeochemical Cycles* 6: 185–198.

Freeman KH and Pagani M (2005) Alkenone-based estimates of past CO_2 levels: A consideration of their utility based on an analysis of uncertainties. In: Ehleringer JR, Cerling TE, and Dearing MD (eds.) *A History of Atmospheric CO_2 and Its Effects on Plants, Animals, and Ecosystems*, pp. 35–61. New York: Springer.

Fry B and Wainwright SC (1991) Diatom sources of ^{13}C-rich carbon in marine food webs. *Marine Ecology Progress Series* 76: 149–157.

Gaffin SR (1987) Ridge volume dependence on seafloor generation rate and inversion using long term sealevel change. *American Journal of Science* 287: 596–611.

Garrels RM and Lerman A (1984) Coupling of the sedimentary sulfur and carbon cycles-an improved model. *American Journal of Science* 284: 989–1007.

Garrels RM and Mackenzie FT (1971) *Evolution of Sedimentary Rocks*. New York: Norton.

Garrels RM and Perry EA (1974) Cycling of carbon, sulfur, and oxygen through geologic time. In: Goldberg ED (ed.) *The Sea*, pp. 303–316. New York: Wiley.

Ghosh P, Bhattacharya SK, and Ghosh P (2005) Atmospheric CO_2 during the Late Paleozoic and Mesozoic: Estimates from Indian soils. In: Ehleringer JR, Cerling TE, and Dearing MD (eds.) *A History of Atmospheric CO_2 and Its Effects on Plants, Animals, and Ecosystems*. New York: Springer.

Ghosh P, Bhattacharya SK, and Jani RA (1995) Palaeoclimate and palaeovegetation in central India during the Upper Cretaceous based on stable isotope composition of the palaeosol carbonates. *Palaeogeography, Palaeoclimatology, Palaeoecology* 114: 285–296.

Ghosh P, Ghosh P, and Bhattacharya SK (2001) CO_2 levels in the Late Palaeozoic and Mesozoic atmosphere from soil carbonate and organic matter, Satpura basin, Central India. *Palaeogeography, Palaeoclimatology, Palaeoecology* 170: 219–236.

Gibbs MT, Barron EJ, and Kump LR (1997) An atmospheric pCO_2 threshold for glaciation in the Late Ordovician. *Geology* 25: 447–450.

Gibbs MT, Bice KL, Barron EJ, and Kump LR (2000) Glaciation in the early Paleozoic 'greenhouse': The roles of paleogeography and atmospheric CO_2. In: Huber BT, MacLeod KG, and Wing SL (eds.) *Warm Climates in Earth History*, pp. 386–422. Cambridge: Cambridge University Press.

Gislason SR, Oelkers EH, Eiriksdottir ES, et al. (2009) Direct evidence of the feedback between climate and weathering. *Earth and Planetary Science Letters* 277: 213–222.

Glasspool IJ, Edwards D, and Axe L (2004) Charcoal in the Silurian as evidence for the earliest wildfire. *Geology* 32: 381–383.

Glasspool IJ and Scott AC (2010) Phanerozoic concentrations of atmospheric oxygen reconstructed from sedimentary charcoal. *Nature Geoscience* 3: 627–630.

Goddéris Y, Donnadieu Y, de Vargas C, Pierrehumbert RT, Dromart G, and van de Schootbrugge B (2008) Causal or casual link between the rise of nannoplankton calcification and a tectonically-driven massive decrease in Late Triassic atmospheric CO_2? *Earth and Planetary Science Letters* 267: 247–255.

Gradstein FM, Ogg JG, and Smith AG (2004) *A Geologic Timescale 2004*. Cambridge: Cambridge University Press.

Graham JB, Dudley R, Aguilar NM, and Gans C (1995) Implications of the late Palaeozoic oxygen pulse for physiology and evolution. *Nature* 375: 117–120.

Gray JE, Holroyd GH, van der Lee FM, et al. (2000) The HIC signalling pathway links CO_2 perception to stomatal development. *Nature* 408: 713–716.

Greenwood DR, Scarr MJ, and Christophel DC (2003) Leaf stomatal frequency in the Australian tropical rainforest tree *Neolitsea dealbata* (Lauraceae) as a proxy measure of atmospheric pCO_2. *Palaeogeography, Palaeoclimatology, Palaeoecology* 196: 375–393.

Grein M, Konrad W, Wilde V, Utescher T, and Roth-Nebelsick A (2011) Reconstruction of atmospheric CO_2 during the early Middle Eocene by application of a gas exchange model to fossil plants from the Messel Formation, Germany. *Palaeogeography, Palaeoclimatology, Palaeoecology* 309: 383–391.

Gulbranson EL, Tabor NJ, and Montañez IP (2011) A pedogenic goethite record of soil CO_2 variations as a response to soil moisture content. *Geochimica et Cosmochimica Acta* 75: 7099–7116.

Hansen J, Sato M, Kharecha P, et al. (2008) Target atmospheric CO_2: Where should humanity aim? *Open Atmospheric Science Journal* 2: 217–231.

Hansen KW and Wallmann K (2003) Cretaceous and Cenozoic evolution of seawater composition, atmospheric O_2 and CO_2: A model perspective. *American Journal of Science* 303: 94–148.

Harrison JF, Kaiser A, and VandenBrooks JM (2010) Atmospheric oxygen level and the evolution of insect body size. *Proceedings of the Royal Society of London, Series B* 277: 1937–1946.

Haworth M, Heath J, and McElwain JC (2010) Differences in the response sensitivity of stomatal index to atmospheric CO_2 among four genera of Cupressaceae conifers. *Annals of Botany* 105: 411–418.

Haworth M, Hesselbo SP, McElwain JC, Robinson SA, and Brunt JW (2005) Mid-Cretaceous pCO_2 based on stomata of the extinct conifer *Pseudofrenelopsis* (Cheirolepidiaceae). *Geology* 33: 749–752.

Hayes JM, Popp BN, Takigiku R, and Johnson MW (1989) An isotopic study of biogeochemical relationships between carbonates and organic carbon in the Greenhorn Formation. *Geochimica et Cosmochimica Acta* 53: 2961–2972.

Hemming NG and Hanson GN (1992) Boron isotopic composition and concentration in modern marine carbonates. *Geochimica et Cosmochimica Acta* 56: 537–543.

Henderiks J and Pagani M (2007) Refining ancient carbon dioxide estimates: Significance of coccolithophore cell size for alkenone-based pCO_2 records. *Paleoceanography* 22: PA3202. http://dx.doi.org/10.1029/2006PA001399.

Henderiks J and Pagani M (2008) Coccolithophore cell size and the Paleogene decline in atmospheric CO_2. *Earth and Planetary Science Letters* 269: 575–583.

Herrmann AD, Patzkowsky ME, and Pollard D (2003) Obliquity forcing with 8–12 times preindustrial levels of atmospheric pCO_2 during the Late Ordovician glaciation. *Geology* 31: 485–488.

Herrmann AD, Patzkowsky ME, and Pollard D (2004) The impact of paleogeography, pCO_2, poleward ocean heat transport and sea level change on global cooling during the Late Ordovician. *Palaeogeography, Palaeoclimatology, Palaeoecology* 206: 59–74.

Hetherington AM and Woodward FI (2003) The role of stomata in sensing and driving environmental change. *Nature* 424: 901–908.

Hinga KR, Arthur MA, Pilson MEQ, and Whitaker D (1994) Carbon isotope fractionation by marine phytoplankton in culture: The effects of CO_2 concentration, pH, temperature, and species. *Global Biogeochemical Cycles* 8: 91–102.

Holland HD (1978) *The Chemistry of the Atmosphere and Oceans*. New York: Wiley.

Holland HD (1984) *The Chemical Evolution of the Atmosphere and Oceans*. Princeton, NJ: Princeton University Press.

Hollander DJ and McKenzie JA (1991) CO_2 control on carbon-isotope fractionation during aqueous photosynthesis: A paleo-pCO_2 barometer. *Geology* 19: 929–932.

Hollis CJ, Handley L, Crouch EM, et al. (2009) Tropical sea temperatures in the high-latitude South Pacific during the Eocene. *Geology* 37: 99–102.

Hönisch B, Bijma J, Russell AD, et al. (2003) The influence of symbiont photosynthesis on the boron isotopic composition of foraminifera shells. *Marine Micropaleontology* 49: 87–96.

Hönisch B and Hemming NG (2004) Ground-truthing the boron isotope-paleo-pH proxy in planktonic foraminifera shells: Partial dissolution and shell size effects. *Paleoceanography* 19: PA4010. http://dx.doi.org/10.1029/2004PA001026.

Hönisch B and Hemming NG (2005) Surface ocean pH response to variations in pCO_2 through two full glacial cycles. *Earth and Planetary Science Letters* 236: 305–314.

Hönisch B, Hemming NG, Archer D, Siddall M, and McManus JF (2009) Atmospheric carbon dioxide concentration across the mid-Pleistocene transition. *Science* 324: 1551–1554.

IPCC (2007) In: Solomon S, Qin D, and Manning M (eds.) *Climate Change 2007: The Physical Science Basis, Contribution of Working Group I to the Fourth Assessment Report of the Intergovernmental Panel on Climate Change*. Cambridge: Cambridge University Press.

Isbell JL, Miller MF, Wolfe KL, and Lenaker PA (2003) Timing of late Paleozoic glaciation in Gondwana: Was glaciation responsible for the development of northern hemisphere cyclothems? In: Chan MA and Archer AW (eds.) *Extreme Depositional Environments: Mega End Members in Geologic Time*, pp. 5–24. Boulder, CO: Geological Society of America, Special Paper 340.

Jagniecki E, Lowenstein TK, and Jenkins D (2010) Sodium carbonates: Temperature and pCO_2 indicators for ancient and modern alkaline saline lakes. *Geological Society of America Abstracts with Programs* 42(5): 404 (Paper No. 165–402).

Jasper JP and Hayes JM (1990) A carbon isotope record of CO_2 levels during the late Quaternary. *Nature* 347: 462–464.

Jordan GJ (2011) A critical framework for the assessment of biological palaeoproxies: Predicting past climate and levels of atmospheric CO_2 from fossil leaves. *New Phytologist* 192: 29–44.

Kaiser A, Klok CJ, Socha JJ, Lee W-K, Quinlan MC, and Harrison JF (2007) Increase in tracheal investment with beetle size supports hypothesis of oxygen limitation on insect gigantism. *Proceedings of the National Academy of Sciences of the United States of America* 104: 13198–13203.

Kashiwagi H and Shikazono N (2003) Climate change during Cenozoic inferred from global carbon cycle model including igneous and hydrothermal activities. *Palaeogeography, Palaeoclimatology, Palaeoecology* 199: 167–185.

Kerrick DM (2001) Present and past nonanthropogenic CO_2 degassing from the solid Earth. *Reviews of Geophysics* 39: 565–585.

Kienast M, Calvert SE, Pelejero C, and Grimalt JO (2001) A critical review of marine sedimentary $\delta^{13}C_{org}$-pCO_2 estimates: New palaeorecords from the South China Sea and a revisit of other low-latitude $\delta^{13}C_{org}$-pCO_2 records. *Global Biogeochemical Cycles* 15: 113–127.

Kleidon A (2007) Optimized stomatal conductance and the climate sensitivity to carbon dioxide. *Geophysical Research Letters* 34: L14709. http://dx.doi.org/10.1029/2007GL030342.

Klochko K, Cody GD, Tossell JA, Dera P, and Kaufman AJ (2009) Re-evaluating boron speciation in biogenic calcite and aragonite using ^{11}B MAS NMR. *Geochimica et Cosmochimica Acta* 73: 1890–1900.

Klochko K, Kaufman AJ, Yao WS, Byrne RH, and Tossell JA (2006) Experimental measurement of boron isotope fractionation in seawater. *Earth and Planetary Science Letters* 248: 276–285.

Koch PL, Zachos JC, and Gingerich PD (1992) Correlation between isotope records in marine and continental carbon reservoirs near the Palaeocene/Eocene boundary. *Nature* 358: 319–322.

Konrad W, Roth-Nebelsick A, and Grein M (2008) Modelling of stomatal density response to atmospheric CO_2. *Journal of Theoretical Biology* 253: 638–658.

Kump LR, Arthur MA, Patzkowsky ME, Gibbs MT, Pinkus DS, and Sheenan PM (1999) A weathering hypothesis for glaciation at high atmospheric pCO_2 during the Late Ordovician. *Palaeoclimatology, Palaeogeography, Palaeoecology* 152: 173–187.

Kürschner WM (1997) The anatomical diversity of recent and fossil leaves of the durmast oak (*Quercus petraea* Lieblein/*Q. pseudocastanea* Goeppert)-implications for their use as biosensors of palaeoatmospheric CO_2 levels. *Review of Palaeobotany and Palynology* 96: 1–30.

Kürschner WM, Kvacek Z, and Dilcher DL (2008) The impact of Miocene atmospheric carbon dioxide fluctuations on climate and the evolution of terrestrial ecosystems. *Proceedings of the National Academy of Sciences of the United States of America* 105: 449–453.

Kürschner WM, van der Burgh J, Visscher H, and Dilcher DL (1996) Oak leaves as biosensors of late Neogene and early Pleistocene paleoatmospheric CO_2 concentrations. *Marine Micropaleontology* 27: 299–312.

Kürschner WM, Wagner F, Dilcher DL, and Visscher H (2001) Using fossil leaves for the reconstruction of Cenozoic paleoatmospheric CO_2 concentrations. In: Gerhard LC, Harrison WE, and Hanson BM (eds.) *Geological Perspectives of Global Climate Change*, pp. 169–189. Tulsa, OK: The American Association of Petroleum Geologists.

Lake JA, Quick WP, Beerling DJ, and Woodward FI (2001) Signals from mature to new leaves. *Nature* 411: 154.

Lake JA, Woodward FI, and Quick WP (2002) Long-distance CO_2 signalling in plants. *Journal of Experimental Botany* 53: 183–193.

Lane N (2002) *Oxygen: The Molecule That Made the World*. Oxford: Oxford University Press.

Le Hir G, Donnadieu Y, Goddéris Y, Meyer-Berthaud B, Ramstein G, and Blakey RC (2011) The climate change caused by the land plant invasion in the Devonian. *Earth and Planetary Science Letters* 310: 203–212.

Lee YI (1999) Stable isotopic composition of calcic paleosols of the Early Cretaceous Hasandong Formation, southeastern Korea. *Palaeogeography, Palaeoclimatology, Palaeoecology* 150: 123–133.

Lee YI and Hisada K (1999) Stable isotopic composition of pedogenic carbonates of the Early Cretaceous Shimonoseki Subgroup, western Honshu, Japan. *Palaeogeography, Palaeoclimatology, Palaeoecology* 153: 127–138.

Leier A, Quade J, DeCelles P, and Kapp P (2009) Stable isotopic results from paleosol carbonate in South Asia: Paleoenvironmental reconstructions and selective alteration. *Earth and Planetary Science Letters* 279: 242–254.

Lemarchand D, Gaillardet J, Lewin É, and Allègre CJ (2000) The influence of rivers on marine boron isotopes and implications for reconstructing past ocean pH. *Nature* 408: 951–954.

Lemarchand D, Gaillardet J, Lewin É, and Allègre CJ (2002) Boron isotope systematics in large rivers: Implications for the marine boron budget and paleo-pH reconstruction over the Cenozoic. *Chemical Geology* 190: 123–140.

Liu Y and Tossell JA (2005) Ab initio molecular orbital calculations for boron isotope fractionations on boric acids and borates. *Geochimica et Cosmochimica Acta* 69: 3995–4006.

Lowenstein TK and Demicco RV (2006) Elevated Eocene atmospheric CO_2 and its subsequent decline. *Science* 313: 1928.

Lunt DJ, Haywood AM, Schmidt GA, Salzmann U, Valdes PJ, and Dowsett HJ (2010) Earth system sensitivity inferred from Pliocene modelling and data. *Nature Geoscience* 3: 60–64.

McAlester AL (1970) Animal extinctions, oxygen consumption, and atmospheric history. *Journal of Paleontology* 44: 405–409.

McElwain JC (1998) Do fossil plants signal palaeoatmospheric CO_2 concentration in the geological past? *Philosophical Transactions of the Royal Society of London* B 353: 83–96.

McElwain JC, Beerling DJ, and Woodward FI (1999) Fossil plants and global warming at the Triassic-Jurassic boundary. *Science* 285: 1386–1390.

McElwain JC and Chaloner WG (1995) Stomatal density and index of fossil plants track atmospheric carbon dioxide in the Palaeozoic. *Annals of Botany* 76: 389–395.

McElwain JC, Mayle FE, and Beerling DJ (2002) Stomatal evidence for a decline in atmospheric CO_2 concentration during the Younger Dryas stadial: A comparison with Antarctic ice core records. *Journal of Quaternary Science* 17: 21–29.

McElwain JC, Wade-Murphy J, and Hesselbo SP (2005) Changes in carbon dioxide during an oceanic anoxic event linked to intrusion into Gondwana coals. *Nature* 435: 479–482.

Montañez IP, Tabor NJ, Niemeier D, et al. (2007) CO_2-forced climate and vegetation instability during late Paleozoic deglaciation. *Science* 315: 87–91.

Mora CI, Driese SG, and Colarusso LA (1996) Middle and Late Paleozoic atmospheric CO_2 levels from soil carbonate and organic matter. *Science* 271: 1105–1107.

Moulten KL and Berner RA (1998) Quantification of the effect of plants on weathering: Studies in Iceland. *Geology* 26: 895–898.

Moulton KL, West J, and Berner RA (2000) Solute flux and mineral mass balance approaches to the quantification of plant effects on silicate weathering. *American Journal of Science* 300: 539–570.

Muchez P, Peeters C, Keppens E, and Viaene WA (1993) Stable isotopic composition of paleosols in the Lower Visan of eastern Belgium: Evidence of evaporation and soil-gas CO_2. *Chemical Geology* 106: 389–396.

Ni Y, Foster GL, Bailey T, et al. (2007) A core top assessment of proxies for the ocean carbonate system in surface-dwelling foraminifers. *Paleoceanography* 22: PA3212. http://dx.doi.org/10.1029/2006PA001337.

Ni Y, Foster GL, and Elliott T (2010) The accuracy of $\delta^{11}B$ measurements of foraminifers. *Chemical Geology* 274: 187–195.

Nordt L, Atchley S, and Dworkin S (2002) Paleosol barometer indicates extreme fluctuations in atmospheric CO_2 across the Cretaceous-Tertiary boundary. *Geology* 30: 703–706.

Nordt L, Atchley S, and Dworkin S (2003) Terrestrial evidence for two greenhouse events in the latest Cretaceous. *GSA Today* 13(12): 4–9.

Otto-Bliesner BL (1995) Continental drift, runoff and weathering feedbacks: Implications from climate model experiments. *Journal of Geophysical Research* 100: 11537–11548.

Pagani M (2002) The alkenone-CO_2 proxy and ancient atmospheric carbon dioxide. *Philosophical Transactions of the Royal Society of London, Series A* 360: 609–632.

Pagani M, Arthur MA, and Freeman KH (1999a) Miocene evolution of atmospheric carbon dioxide. *Paleoceanography* 14: 273–292.

Pagani M, Caldeira K, Berner R, and Beerling DJ (2009) The role of terrestrial plants in limiting atmospheric CO_2 decline over the past 24 million years. *Nature* 460: 85–88.

Pagani M, Freeman KH, and Arthur MA (1999b) Late Miocene atmospheric CO_2 concentrations and the expansion of C_4 grasses. *Science* 285: 876–879.

Pagani M, Freeman KH, and Arthur MA (2000) Isotope analyses of molecular and total organic carbon from Miocene sediments. *Geochimica et Cosmochimica Acta* 64: 37–49.

Pagani M, Huber M, Liu Z, et al. (2011) The role of carbon dioxide during the onset of Antarctic glaciation. *Science* 334: 1261–1264.

Pagani M, Lemarchand D, Spivack A, and Gaillardet J (2005a) A critical evaluation of the boron isotope-*p*H proxy: The accuracy of ancient ocean *p*H estimates. *Geochimica et Cosmochimica Acta* 69: 953–961.

Pagani M, Liu Z, LaRiviere J, and Ravelo AC (2010) High Earth-system climate sensitivity determined from Pliocene carbon dioxide concentrations. *Nature Geoscience* 3: 27–30.

Pagani M, Zachos JC, Freeman KH, Tipple B, and Bohaty S (2005b) Marked decline in atmospheric carbon dioxide concentrations during the Paleogene. *Science* 309: 600–603.

Palmer MR, Pearson PN, and Cobb SJ (1998) Reconstructing past ocean pH-depth profiles. *Science* 282: 1468–1471.

Paris G, Gaillardet J, and Louvet P (2010) Geological evolution of seawater boron isotopic composition recorded in evaporites. *Geology* 38: 1035–1038.

Park J and Royer DL (2011) Geologic constraints on the glacial amplification of Phanerozoic climate sensitivity. *American Journal of Science* 311: 1–26.

Passalia MG (2009) Cretaceous pCO_2 estimation from stomatal frequency analysis of gymnosperm leaves of Patagonia, Argentina. *Palaeogeography, Palaeoclimatology, Palaeoecology* 273: 17–24.

Pearson PN, Ditchfield PW, Singano J, et al. (2001) Warm tropical sea surface temperatures in the Late Cretaceous and Eocene epochs. *Nature* 413: 481–487.

Pearson PN, Foster GL, and Wade BS (2009) Atmospheric carbon dioxide through the Eocene-Oligocene climate transition. *Nature* 461: 1110–1113.

Pearson PN and Palmer MR (1999) Middle Eocene seawater pH and atmospheric carbon dioxide concentrations. *Science* 284: 1824–1826.

Pearson PN and Palmer MR (2000) Atmospheric carbon dioxide concentrations over the past 60 million years. *Nature* 406: 695–699.

Platt NH (1989) Lacustrine carbonates and pedogenesis: Sedimentology and origin of palustrine deposits from the Early Cretaceous Rupelo Formation, W. Cameros Basin, N. Spain. *Sedimentology* 36: 665–684.

Popp BN, Laws EA, Bidigare RR, Dore JE, Hanson KL, and Wakeham SG (1998) Effect of phytoplankton cell geometry on carbon isotopic fractionation. *Geochimica et Cosmochimica Acta* 62: 69–77.

Popp BN, Takigiku R, Hayes JM, Louda JW, and Baker EW (1989) The post-Paleozoic chronology and mechanism of ^{13}C depletion in primary marine organic matter. *American Journal of Science* 289: 436–454.

Poussart PF, Weaver AJ, and Barnes CR (1999) Late Ordovician glaciation under high atmospheric CO_2: A coupled model analysis. *Paleoceanography* 14: 542–558.

Price GD, McKenzie JE, Pilcher JR, and Hoper ST (1997) Carbon-isotope variation in *Sphagnum* from hummock-hollow complexes: Implications for Holocene climate reconstruction. *The Holocene* 7: 229–233.

Prochnow SJ, Nordt LC, Atchley SC, and Hudec MR (2006) Multi-proxy paleosol evidence for middle and late Triassic climate trends in eastern Utah. *Palaeogeography, Palaeoclimatology, Palaeoecology* 232: 53–72.

Prokoph A, Shields GA, and Veizer J (2008) Compilation and time-series analysis of a marine carbonate $\delta^{18}O$, $\delta^{13}C$, and $^{87}Sr/^{86}Sr$ and $\delta^{34}S$ database through Earth history. *Earth-Science Reviews* 87: 113–133.

Quan C, Sun C, Sun Y, and Sun G (2009) High resolution estimates of paleo-CO_2 levels through the Campanian (Late Cretaceous) based on *Ginkgo* cuticles. *Cretaceous Research* 30: 424–428.

Quast A, Hoefs J, and Paul J (2006) Pedogenic carbonates as a proxy for palaeo-CO_2 in the Palaeozoic atmosphere. *Palaeogeography, Palaeoclimatology, Palaeoecology* 242: 110–125.

Rahmstorf S, Archer D, Ebel DS, et al. (2004) Cosmic rays, carbon dioxide, and climate. *Eos, Transactions, American Geophysical Union*, 38–41 85.

Retallack GJ (2001) A 300-million-year record of atmospheric carbon dioxide from fossil plant cuticles. *Nature* 411: 287–290.

Retallack GJ (2002) Carbon dioxide and climate over the past 300 Myr. *Philosophical Transactions of the Royal Society of London A* 360: 659–673.

Retallack GJ (2009a) Greenhouse crises of the past 300 million years. *Geological Society of America Bulletin* 121: 1441–1455.

Retallack GJ (2009b) Refining a pedogenic-carbonate CO_2 paleobarometer to quantify a middle Miocene greenhouse spike. *Palaeogeography, Palaeoclimatology, Palaeoecology* 281: 57–65.

Rice SK and Giles L (1996) The influence of water content and leaf anatomy on carbon isotope discrimination and photosynthesis in *Sphagnum*. *Plant, Cell and Environment* 19: 118–124.

Ridgwell A and Zeebe RE (2005) The role of the global carbonate cycle in the regulation and evolution of the Earth system. *Earth and Planetary Science Letters* 234: 299–315.

Roberts CD and Tripati AK (2009) Modeled reconstructions of the oceanic carbonate system for different histories of atmospheric carbon dioxide during the last 20 Ma. *Global Biogeochemical Cycles* 23: GB1011. http://dx.doi.org/10.1029/2008GB003310.

Robinson JM (1990) Lignin, land plants, and fungi: Biological evolution affecting Phanerozoic oxygen balance. *Geology* 15: 607–610.

Robinson JM (1991) Phanerozoic atmospheric reconstructions: A terrestrial perspective. *Global and Planetary Change* 5: 51–62.

Robinson SA, Andrews JE, Hesselbo SP, et al. (2002) Atmospheric pCO_2 and depositional environment from stable-isotope geochemistry of calcrete nodules (Barremian, Lower Cretaceous, Wealden Beds, England). *Journal of the Geological Society of London* 159: 215–224.

Rothman DH (2002) Atmospheric carbon dioxide levels for the last 500 million years. *Proceedings of the National Academy of Sciences of the United States of America* 99: 4167–4171.

Roth-Nebelsick A and Konrad W (2003) Assimilation and transpiration capabilities of rhyniophytic plants from the Lower Devonian and their implications for paleoatmospheric CO_2 concentration. *Palaeogeography, Palaeoclimatology, Palaeoecology* 202: 153–178.

Royer DL (1999) Depth to pedogenic carbonate horizon as a paleoprecipitation indicator? *Geology* 27: 1123–1126.

Royer DL (2001) Stomatal density and stomatal index as indicators of paleoatmospheric CO_2 concentration. *Review of Palaeobotany and Palynology* 114: 1–28.

Royer DL (2003) Estimating latest Cretaceous and Tertiary atmospheric CO_2 concentration from stomatal indices. In: Wing SL, Gingerich PD, Schmitz B, and Thomas E (eds.) *Causes and Consequences of Globally Warm Climates in the Early Paleogene*, pp. 79–93. Boulder, CO: Geological Society of America Special Paper 369.

Royer DL (2006) CO_2-forced climate thresholds during the Phanerozoic. *Geochimica et Cosmochimica Acta* 70: 5665–5675.

Royer DL (2010) Fossil soils constrain ancient climate sensitivity. *Proceedings of the National Academy of Sciences of the United States of America* 107: 517–518.

Royer DL, Berner RA, and Beerling DJ (2001a) Phanerozoic CO_2 change: Evaluating geochemical and paleobiological approaches. *Earth-Science Reviews* 54: 349–392.

Royer DL, Berner RA, Montañez IP, Tabor NJ, and Beerling DJ (2004) CO_2 as a primary driver of Phanerozoic climate. *GSA Today* 14(3): 4–10.

Royer DL, Berner RA, and Park J (2007) Climate sensitivity constrained by CO_2 concentrations over the past 420 million years. *Nature* 446: 530–532.

Royer DL, Wing SL, Beerling DJ, et al. (2001b) Paleobotanical evidence for near present-day levels of atmospheric CO_2 during part of the Tertiary. *Science* 292: 2310–2313.

Rundgren M and Beerling D (1999) A Holocene CO_2 record from the stomatal index of sub-fossil *Salix herbacea* L. leaves from northern Sweden. *The Holocene* 9: 509–513.

Rundgren M and Beerling D (2003) Fossil leaves: Effective bioindicators of ancient CO_2 levels? *Geochemistry, Geophysics, Geosystems* 4(7): 1058. http://dx.doi.org/10.1029/2002GC000463.

Rundgren M, Björck S, and Hammarlund D (2005) Last interglacial atmospheric CO_2 changes from stomatal index data and their relation to climate variations. *Global and Planetary Change* 49: 47–62.

Runkel AC, Mackey TJ, Cowan CA, and Fox DL (2010) Tropical shoreline ice in the late Cambrian: Implications for Earth's climate between the Cambrian Explosion and the Great Ordovician Biodiversification Event. *GSA Today* 20(11): 4–10.

Rustad JR, Bylaska EJ, Jackson VE, and Dixon DA (2010) Calculation of boron-isotope fractionation between $B(OH)_3(aq)$ and $B(OH)_4^-(aq)$. *Geochimica et Cosmochimica Acta* 74: 2843–2850.

Rustad JR and Zarzycki P (2008) Calculation of site-specific carbon-isotope fractionation in pedogenic oxide minerals. *Proceedings of the National Academy of Sciences of the United States of America* 105: 10297–10301.

Saltzman MR, Young SA, Kump LR, Gill BC, Lyons TW, and Runnegar B (2011) Pulse of atmospheric oxygen during the late Cambrian. *Proceedings of the National Academy of Sciences of the United States of America* 108: 3876–3881.

Sandler A (2006) Estimates of atmospheric CO_2 levels during the mid-Turonian derived from stable isotope composition of paleosol calcite from Israel. In: Alonso-Zarza AM and Tanner LH (eds.) *Paleoenvironmental Record and Applications of Calcretes and Palustrine Carbonates*, pp. 75–88. Boulder, CO: Geological Society of America, Special Paper 416.

Sanyal A, Hemming NG, Broecker WS, Lea DW, Spero HJ, and Hanson GN (1996) Oceanic *p*H control on the boron isotopic composition of foraminifera: Evidence from culture experiments. *Paleoceanography* 11: 513–517.

Sanyal A, Hemming NG, Hanson GN, and Broecker WS (1995) Evidence for a higher pH in the glacial ocean from boron isotopes in foraminifera. *Nature* 373: 234–236.

Sarkar A, Sarangi S, Bhattacharya SK, and Ray AK (2003) Carbon isotopes across the Eocene-Oligocene boundary sequence of Kutch, western India: Implications to oceanic productivity and pCO_2 change. *Geophysical Research Letters* 30: 1588. http://dx.doi.org/10.1029/2002GL016541.

Schaller MF, Wright JD, and Kent DV (2011) Atmospheric P_{CO2} perturbations associated with the Central Atlantic Magmatic Province. *Science* 331: 1404–1409.

Schroeder PA, Austin JC, and Dowd JF (2006) Estimating long-term soil respiration rates from carbon isotopes occluded in gibbsite. *Geochimica et Cosmochimica Acta* 70: 5692–5697.

Scott AC (2000) The pre-Quaternary history of fire. *Palaeogeography, Palaeoclimatology, Palaeoecology* 164: 297–345.

Scott AC and Glasspool IJ (2006) The diversification of Paleozoic fire systems and fluctuations in atmospheric oxygen concentration. *Proceedings of the National Academy of Sciences of the United States of America* 103: 10861–10865.

Seki O, Foster GL, Schmidt DN, Mackensen A, Kawamura K, and Pancost RD (2010) Alkenone and boron-based Pliocene *p*CO2 records. *Earth and Planetary Science Letters* 292: 201–211.

Seton M, Gaina C, Müller RD, and Heine C (2009) Mid-Cretaceous seafloor spreading pulse: Fact or fiction? *Geology* 37: 687–690.

Sheldon ND and Tabor NJ (2009) Quantitative paleoenvironmental and paleoclimatic reconstruction using paleosols. *Earth-Science Reviews* 95: 1–52.

Simon L, Lécuyer C, Maréchal C, and Coltice N (2006) Modelling the geochemical cycle of boron: Implications for the long-term $\delta^{11}B$ evolution of seawater and oceanic crust. *Chemical Geology* 225: 61–76.

Sinha A and Stott LD (1994) New atmospheric pCO_2 estimates from paleosols during the late Paleocene/early Eocene global warming interval. *Global and Planetary Change* 9: 297–307.

Smith RY, Greenwood DR, and Basinger JF (2010) Estimating paleoatmospheric pCO_2 during the Early Eocene Climatic Optimum from stomatal frequency of *Ginkgo*, Okanagan Highlands, British Columbia, Canada. *Palaeogeography, Palaeoclimatology, Palaeoecology* 293: 120–131.

Spivack AJ and You C-F (1997) Boron isotopic geochemistry of carbonates and pore waters, Ocean Drilling Program Site 851. *Earth and Planetary Science Letters* 152: 113–122.

Spivack AJ, You C-F, and Smith HJ (1993) Foraminiferal boron isotope ratios as a proxy for surface ocean pH over the past 21 Myr. *Nature* 363: 149–151.

Steinthorsdottir M, Jeram AJ, and McElwain JC (2011) Extremely elevated CO_2 concentrations at the Triassic/Jurassic boundary. *Palaeogeography, Palaeoclimatology, Palaeoecology* 308: 418–432.

Stults DZ, Wagner-Cremer F, and Axsmith BJ (2011) Atmospheric paleo-CO_2 estimates based on *Taxodium distichum* (Cupressaceae) fossils from the Miocene and Pliocene of eastern North America. *Palaeogeography, Palaeoclimatology, Palaeoecology* 309: 327–332.

Suchecki RK, Hubert JF, and Birney de Wet CC (1988) Isotopic imprint of climate and hydrogeochemistry on terrestrial strata of the Triassic-Jurassic Hartford and Fundy rift basins. *Journal of Sedimentary Petrology* 58: 801–811.

Sun B, Dilcher DL, Beerling DJ, Zhang C, Yan D, and Kowalski E (2003) Variation in *Ginkgo biloba* L. leaf characters across a climatic gradient in China. *Proceedings of the National Academy of Sciences of the United States of America* 100: 7141–7146.

Sun B, Xiao L, Xie S, et al. (2007) Quantitative analysis of paleoatmospheric CO_2 level based on stomatal characters of fossil *Ginkgo* from Jurassic to Cretaceous in China. *Acta Geologica Sinica* 81: 931–939.

Tabor NJ and Yapp CJ (2005) Coexisting goethite and gibbsite from a high-paleolatitude (55°N) Late Paleocene laterite: Concentration and $^{13}C/^{12}C$ ratios of occluded CO_2 and associated organic matter. *Geochimica et Cosmochimica Acta* 69: 5495–5510.

Tabor NJ, Yapp CJ, and Montañez IP (2004) Goethite, calcite, and organic matter from Permian and Triassic soils: Carbon isotopes and CO_2 concentrations. *Geochimica et Cosmochimica Acta* 68: 1503–1517.

Tajika E (1998) Climate change during the last 150 million years: Reconstruction from a carbon cycle model. *Earth and Planetary Science Letters* 160: 695–707.

Tanner LH, Hubert JF, Coffey BP, and McInerney DP (2001) Stability of atmospheric CO_2 levels across the Triassic/Jurassic boundary. *Nature* 411: 675–677.

Taylor LL, Leake JR, Quirk J, Hardy K, Banwart SA, and Beerling DJ (2009) Biological weathering and the long-term carbon cycle: Integrating mycorrhizal evolution and function into the current paradigm. *Geobiology* 7: 171–191.

Tipple BJ, Meyers SR, and Pagani M (2010) Carbon isotope ratio of Cenozoic CO_2: A comparative evaluation of available geochemical proxies. *Paleoceanography* 25: PA3202. http://dx.doi.org/10.1029/2009PA001851.

Tripati AK, Roberts CD, and Eagle RA (2009) Coupling of CO_2 and ice sheet stability over major climate transitions of the last 20 million years. *Science* 326: 1394–1397.

Tyrrell T and Zeebe RE (2004) History of carbonate ion concentration over the last 100 million years. *Geochimica et Cosmochimica Acta* 68: 3521–3530.

Urey HC (1952) *The Planets: Their Origin and Development*. New Haven, CT: Yale University Press.

Van Cappellen P and Ingall ED (1996) Redox stabilization of the atmosphere and oceans by phosphorus-limited marine productivity. *Science* 271: 493–496.

van der Burgh J, Visscher H, Dilcher DL, and Kürschner WM (1993) Paleoatmospheric signatures in Neogene fossil leaves. *Science* 260: 1788–1790.

VandenBrooks J, Munoz E, Weed M, Ford C, Harrison M, and Harrison J (2012) Impacts of paleo-oxygen levels on the size, development, reproduction, and tracheal systems of *Blatella germanica*. *Evolutionary Biology* 39: 83–93.

Vaughan APM (2007) Climate and geology – A Phanerozoic perspective. In: Williams M, Haywood AM, Gregory FJ, and Schmidt DN (eds.) *Deep-Time Perspectives on Climate Change: Marrying the Signal from Computer Models and Biological Proxies*, pp. 5–59. London: The Geological Society and The Micropalaeontological Society, Special Publications.

Veizer J, Ala D, Azmy K, et al. (1999) $^{87}Sr/^{86}Sr$, $\delta^{13}C$ and $\delta^{18}O$ evolution of Phanerozoic seawater. *Chemical Geology* 161: 59–88.

Vengosh A, Kolodny Y, Starinsky A, Chivas AR, and McCulloch MT (1991) Coprecipitation and isotopic fractionation of boron in modern biogenic carbonates. *Geochimica et Cosmochimica Acta* 55: 2901–2910.

Vörding B and Kerp H (2008) Stomatal indices of *Peltaspermum martinsii* (Pteridospermopsida, Peltaspermaceae) from the Upper Permian Bletterbach Gorge and their possible applicability as CO_2 proxies. *Neues Jahrbuch Für Geologie und Paläontologie Abhandlungen* 248: 245–255.

Walker JCG, Hays PB, and Kasting JF (1981) A negative feedback mechanism for the long-term stabilization of Earth's surface temperature. *Journal of Geophysical Research* 86: 9776–9782.

Wallmann K (2001) Controls on the Cretaceous and Cenozoic evolution of seawater composition, atmospheric CO_2 and climate. *Geochimica et Cosmochimica Acta* 65: 3005–3025.

Wallmann K (2004) Impact of atmospheric CO_2 and galactic cosmic radiation on Phanerozoic climate change and the marine $\delta^{18}O$ record. *Geochemistry, Geophysics, Geosystems* 5: Q06004. http://dx.doi.org/10.1029/2003GC000683.

Wan CB, Wang DH, Zhu ZP, and Quan C (2011) Trend of Santonian (Late Cretaceous) atmospheric CO_2 and global mean land surface temperature: Evidence from plant fossils. *Science China Earth Sciences* 54: 1338–1345.

Wara MW, Delaney ML, Bullen TD, and Ravelo AC (2003) Possible roles of pH, temperature, and partial dissolution in determining boron concentration and isotopic composition in planktonic foraminifera. *Paleoceanography* 18(4): 1100. http://dx.doi.org/10.1029/2002PA000797.

Weart SR (2003) *The Discovery of Global Warming*. Cambridge: Harvard University Press.

White JWC, Ciais P, Figge RA, Kenny R, and Markgraf V (1994) A high-resolution record of atmospheric CO_2 content from carbon isotopes in peat. *Nature* 367: 153–156.

Wildman RA, Berner RA, Petsch ST, et al. (2004a) The weathering of sedimentary organic matter as a control on atmospheric O_2: I. Analysis of a black shale. *American Journal of Science* 304: 234–249.

Wildman RA, Hickey LJ, Dickinson MB, et al. (2004b) Burning of forest materials under late Paleozoic high atmospheric oxygen levels. *Geology* 32: 457–460.

Wilkinson BH and Walker JCG (1989) Phanerozoic cycling of sedimentary carbonate. *American Journal of Science* 289: 525–548.

Willis KJ and McElwain JC (2002) *The Evolution of Plants*. New York: Oxford University Press.

Woodward FI (1986) Ecophysiological studies on the shrub *Vaccinium myrtillus* L. taken from a wide altitudinal range. *Oecologia* 70: 580–586.

Woodward FI (1987) Stomatal numbers are sensitive to increases in CO_2 from pre-industrial levels. *Nature* 327: 617–618.

Woodward FI and Bazzaz FA (1988) The responses of stomatal density to CO_2 partial pressure. *Journal of Experimental Botany* 39: 1771–1781.

Worsley TR and Kidder DL (1991) 1st-order coupling of paleogeography and CO_2 with global surface temperature and its latitudinal contrast. *Geology* 19: 1161–1164.

Wynn JG (2003) Towards a physically based model of CO_2-induced stomatal frequency response. *New Phytologist* 157: 391–398.

Wynn JG (2007) Carbon isotope fractionation during decomposition of organic matter in soils and paleosols: Implications for paleoecological interpretations of paleosols. *Palaeogeography, Palaeoclimatology, Palaeoecology* 251: 437–448.

Yan DF, Sun BN, Xie SP, Li XC, and Wen WW (2009) Response to paleotemperature CO_2 concentration of *Solenites vimineus* (Phillips) Harris (Ginkgophyta) from the Middle Jurassic of the Yaojie Basin, Gansu Province, China. *Science in China Series D: Earth Sciences* 52: 2029–2039.

Yapp CJ (1987) A possible goethite-iron(III) carbonate solid solution and the determination of CO_2 partial pressures in low-temperature geologic systems. *Chemical Geology* 64: 259–268.

Yapp CJ (2004) $Fe(CO_3)OH$ in goethite from a mid-latitude North American Oxisol: Estimate of atmospheric CO_2 concentration in the Early Eocene "climatic optimum". *Geochimica et Cosmochimica Acta* 68: 935–947.

Yapp CJ and Poths H (1991) $^{13}C/^{12}C$ ratios of the Fe(III) carbonate component in natural goethites. In: Taylor HP, O'Neil JR, and Kaplan IR (eds.) *Stable Isotope Geochemistry: A Tribute to Samuel Epstein*, pp. 257–270. San Antonio: The Geochemical Society, Special Publication 3.

Yapp CJ and Poths H (1992) Ancient atmospheric CO_2 pressures inferred from natural goethites. *Nature* 355: 342–344.

Yapp CJ and Poths H (1996) Carbon isotopes in continental weathering environments and variations in ancient atmospheric CO_2 pressure. *Earth and Planetary Science Letters* 137: 71–82.

Young SA, Saltzman MR, Ausich WI, Desrochers A, and Kaljo D (2010) Did changes in atmospheric CO_2 coincide with latest Ordovician glacial-interglacial cycles? *Palaeogeography, Palaeoclimatology, Palaeoecology* 296: 376–388.

Yu J, Elderfield H, and Hönisch B (2007) B/Ca in planktonic foraminifera as a proxy for surface seawater pH. *Paleoceanography* 22: PA2202. http://dx.doi.org/10.1029/2006PA001347.

Yu J, Foster GL, Elderfield H, Broecker WS, and Clark E (2010) An evaluation of benthic foraminiferal B/Ca and $\delta^{11}B$ for deep ocean carbonate ion and pH reconstructions. *Earth and Planetary Science Letters* 293: 114–120.

Zachos JC, Dickens GR, and Zeebe RE (2008) An early Cenozoic perspective on greenhouse warming and carbon-cycle dynamics. *Nature* 451: 279–283.

Zeebe RE (2005) Stable boron isotope fractionation between dissolved $B(OH)_3$ and $B(OH)_4^-$. *Geochimica et Cosmochimica Acta* 69: 2753–2766.

Zeebe RE and Caldeira K (2008) Close mass balance of long-term carbon fluxes from ice-core CO_2 and ocean chemistry records. *Nature Geoscience* 1: 312–315.

Zeebe RE, Wolf-Gladrow DA, Bijma J, and Hönisch B (2003) Vital effects in foraminifera do not compromise the use of $\delta^{11}B$ as a paleo-*p*H indicator: Evidence from modeling. *Paleoceanography* 18(2): 1043. http://dx.doi.org/10.1029/2003PA000881.